Sensory and Motor Systems

Stress Increases Peripheral Axon Growth and Regeneration through Glucocorticoid Receptor-Dependent Transcriptional Programs

Jessica K. Lerch,[1,*] Jessica K. Alexander,[1,*] Kathryn M. Madalena,[1] Dario Motti,[2,4] Tam Quach,[1] Akhil Dhamija,[1] Alicia Zha,[1] John C. Gensel,[1,5] Jeanette Webster Marketon,[6] Vance P. Lemmon,[2] John L. Bixby,[2,3] and Phillip G. Popovich[1]

DOI:http://dx.doi.org/10.1523/ENEURO.0246-17.2017

[1]Center for Brain and Spinal Cord Repair, Department of Neuroscience, Wexner Medical Center at the Ohio State University, Columbus, OH 43210, [2]The Miami Project to Cure Paralysis, Department of Neurological Surgery, The University of Miami, Miami, FL 33136, [3]Department of Pharmacology, The University of Miami, Miami, FL 33136, [4]Center for Gene Therapy, The Research Institute at Nationwide Children's Hospital, Columbus, OH 43205, [5]Spinal Cord and Brain Injury Research Center, Department of Physiology, The University of Kentucky, Lexington, KY 40536, [6]SRA International Inc, Beavercreek, OH 45431

Abstract

Stress and glucocorticoid (GC) release are common behavioral and hormonal responses to injury or disease. In the brain, stress/GCs can alter neuron structure and function leading to cognitive impairment. Stress and GCs also exacerbate pain, but whether a corresponding change occurs in structural plasticity of sensory neurons is unknown. Here, we show that in female mice (*Mus musculus*) basal GC receptor (*Nr3c1*, also known as GR) expression in dorsal root ganglion (DRG) sensory neurons is 15-fold higher than in neurons in canonical stress-responsive brain regions (*M. musculus*). In response to stress or GCs, adult DRG neurite growth increases through mechanisms involving GR-dependent gene transcription. *In vivo*, prior exposure to an acute systemic stress increases peripheral nerve regeneration. These data have broad clinical implications and highlight the importance of stress and GCs as novel behavioral and circulating modifiers of neuronal plasticity.

Key words: Key Words: dorsal root ganglia; glucocorticoid receptor; plasticity; stress

Significance Statement

Nerve injury-induced pain affects millions and is a comorbidity factor for individuals living with traumatic spinal cord or peripheral nerve injuries. Pain is associated with aberrant plasticity and sprouting in the injured peripheral and central nervous systems. However, the mechanisms underlying these structural changes are not understood. Here, new data implicate stress hormones (steroids) and GR activation as a novel mechanism underlying enhanced sensory neuron plasticity in injured peripheral nerves. These data also have important implications for the development and care of nerve-injury induced pain, including the use of steroids as a treatment for inflammatory pain.

Introduction

Stress, a ubiquitous and recurrent part of daily life, activates complex regulatory mechanisms in the body that cause glucocorticoids (GCs) to increase in the circulation. GCs are steroid hormones that dramatically affect cell function. They do so mainly by binding to GC receptors (GRs), which act in the nucleus to regulate gene transcription. In the brain, neurons in the cerebral cortex

Received July 14, 2017; accepted July 18, 2017; First published August 11, 2017.
The authors declare no competing financial interests.

Author contributions: J.K.L., J.K.A., D.M., J.C.G., J.W.M., V.P.L., J. L.B., and P.G.P. designed research; J.K.L., J.K.A., K.M.M., D.M., T.Q., A.D., A.Z., J.C.G., and J.W.M. performed research; J.K.L., J.K.A., K.M.M., D.M., T.Q., and J.W.M.

and subcortical structures (e.g., hippocampus, amygdala) express high levels of GRs (Sapolsky et al., 1984) and GCs/stress can modulate their structural integrity. For example, GCs cause dendritic hypertrophy in amygdala neurons (Vyas et al., 2002) and dendritic atrophy in hippocampal neurons (Watanabe et al., 1992; Mitra and Sapolsky, 2008). These structural changes alter long-term potentiation and depression (Kerr et al., 1992; De Kloet et al., 1998; Yang et al., 2004; Ahmed et al., 2006) and are associated with increased anxiety and age-related cognitive impairment (Watanabe et al., 1992; Lupien et al., 1998; Revest et al., 2005). Neurons in the dorsal root ganglia (DRGs) also express GRs (DeLeón et al., 1994) but the relative level of GR expression in DRG compared to brain neurons is unknown. It is also not known whether stress/GCs can affect the structure or function of DRG neurons.

Peripheral nerve injury (e.g., axotomy or nerve ligation) activates transcriptional programs that enhance DRG neuron regenerative growth and sprouting (Smith and Skene, 1997; Neumann and Woolf, 1999). Peripheral nerve injury also causes neuropathic pain (Decosterd and Woolf, 2000; Shields et al., 2003), a condition that may develop because aberrant growth programs are elicited in sensory neurons causing sprouting into the superficial layers of the spinal cord dorsal horn (Woolf et al., 1992; Ondarza et al., 2003; Hughes et al., 2008; Zhang et al., 2015) or the nucleus gracilis and cuneatus (Persson et al., 1995; Ma and Bisby, 1998, 2000). In animal models, stress and GCs enhance nerve injury-induced pain (Wang et al., 2004; Alexander et al., 2009), although the mechanisms underlying these changes in sensation are unknown.

Our new data indicate that GCs act as circulating modifiers of sensory neuron structure and function and that DRG neurons express surprisingly high levels of GRs, even compared to hippocampal neurons, which have been considered the most GR-rich and stress-responsive neurons in the nervous system (Sapolsky et al., 1984). When DRG neurons are isolated from stressed mice and grown *in vitro*, they grow neurites that are both longer and more complex than those that grow from control DRG neurons. These growth-promoting effects of stress can be blocked using GR antagonists, and recapitulated *in vivo* by injecting synthetic GCs into naïve mice before DRG neuron harvest. Stress increases GR nuclear localization in DRG neurons but without markedly increasing the expression of regeneration-associated genes (RAGs). In fact, unlike the ability of nerve injury (e.g., conditioning lesion) to elicit RAG expression (Stam et al., 2007), stress prevents injury-induced increases in RAG expression (*Atf3*, *Ankrd1*, *Sprr1a*) while other potentially novel GR-dependent RAGs (e.g., *Gilz*, *Cebpa*) are increased by stress. Finally, we show that the axon growth-promoting effects of stress/GCs can also be identified *in vivo*. These data highlight the importance of stress and GCs as novel behavioral and circulating modifiers of sensory neuron plasticity, and bring into question whether the inflammation associated with pain should be treated with steroids.

Materials and Methods

Animals

Adult female C57BL/6 mice (Taconic) or *Thy1-GFP-M* mice (Feng et al., 2000) were group housed in standard cages with *ad libitum* access to food and water. Mice were maintained in a vivarium with controlled temperature (~20°C) on a 12/12 h light/dark cycle and assigned randomly to experimental groups after a one week habituation period. All procedures were conducted by protocols approved by The Ohio State University and the University of Miami Institutional Laboratory Animal Care and Use Committee and with the guidelines of the Committee for Research and Ethical Issues of International Association for the Study of Pain.

Western blotting

Mice were sacrificied in accordance to Institutional Animal Care and Use Committee guildelines and DRG cell lysates were prepared by homogenization in 250-μl T-PER Tissue Protein Extraction Reagent (Thermo Fisher, PI-78510) supplemented with protease and phosphatase inhibitors (Halt Cocktails, #87786; Thermo Scientific) immediately after harvest. Following centrifugation (10,000 $\times$ *g* for 5 min), protein concentration was determined using a BCA protein assay kit (Thermo Scientific, PI-23221). Samples (10 μg) were separated on 10% Bis-Tris gels and transferred to a nitrocellulose membrane in a wet-transfer apparatus (Invitrogen). After protein transfer, membranes were incubated with 5% BSA for 1 h at room temperature (RT), then with one of the following primary antibodies (1:200-1:2000): GR #PA1-511A from Thermo Scientific, RRID: AB_2236340; Actin #A1978 from Sigma-Aldrich, RRID: AB_476692, in 5% BSA at 4°C for at least 12 h, and finally with HRP-conjugated anti-rabbit IgG antibody (1:5000-1:15,000; Jackson ImmunoResearch, #111-035-046) in 5% BSA for 1 h at RT. Between incubations, the membrane was washed three times with PBS + 5% Tween for 10 min each. HRP activity was visualized using a chemiluminescent substrate (Thermo Scientific) and signal density quantified with a Kodak Image Station 4000MM Pro (Carestream Health). A ratio of signal density of phosphorylated protein to total protein was calculated. For Figure 1, the amount of DRG GR protein in 10 µg of tissue lysate exceeded the limits of a standard curve dilution produced by recombinant GR; consequently, the loading amount had to be reduced and results are evaluated on the

analyzed data; J.K.L., J.K.A., K.M.M., V.P.L., J.L.B., and P.G.P. wrote the paper.

This work was supported by National Institute of Neurological Disorders and Stroke Grants R01 NS083942 (to P.G.P.) and R01 HD057632 (to V.P.L. and J.L.B.).

*J.K.L. and J.K.A. contributed equally to this work.

Acknowledgments: We thank Kate Zakharova and Perry Delvin for technical assistance.

Correspondence should be addressed to either of the following: Jessica K. Lerch, 460 West 12th Avenue, BRT0696, Columbus, OH 43210, E-mail: lerch.27@osu.edu; or Phillip G. Popovich, 460 West 12th Avenue, BRT694, Columbus, OH 43210, E-mail: popovich.2@osu.edu.

DOI:http://dx.doi.org/10.1523/ENEURO.0246-17.2017

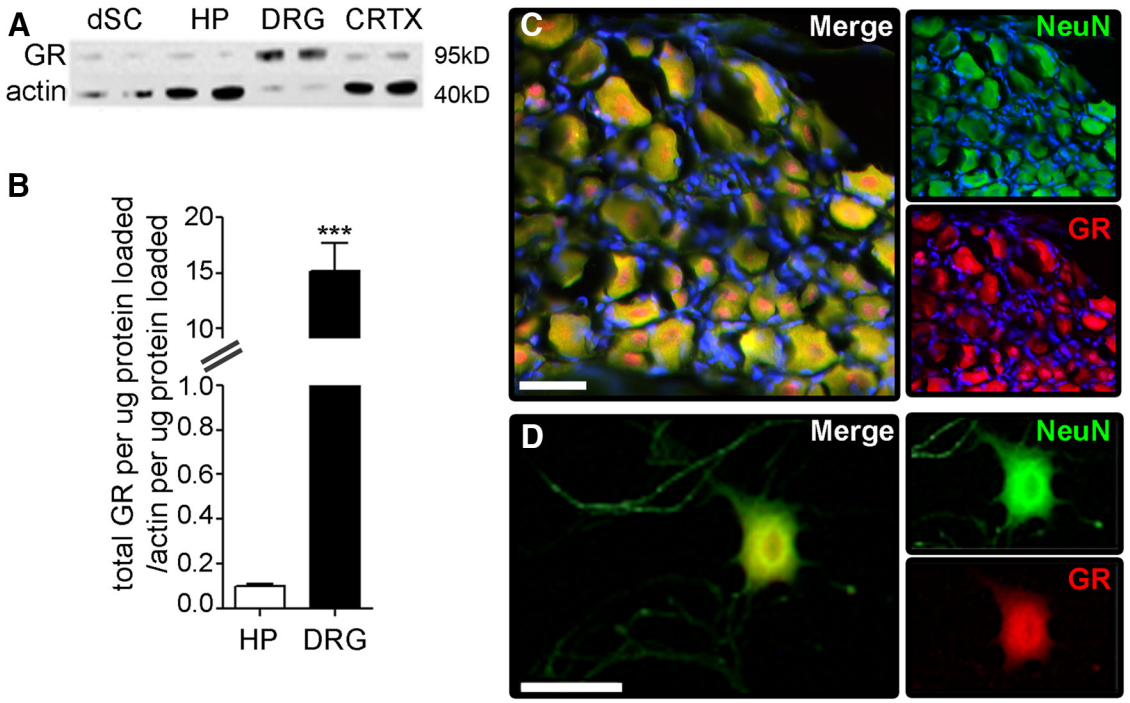

Figure 1. DRG neurons express high levels of GR. ***A***, GR expression was analyzed via Western blotting using protein isolated from homogenates of dorsal spinal cord (dSC), hippocampus (HP), DRG, or cerebral cortex (CRTX). ***B***, GR expression in DRG was >15-fold higher than in hippocampus ($p < 0.0001$); $N = 4$ per group, mean and SEM are shown. ***C***, Immunohistochemical staining for GR (red) in sections of whole DRG or (***D***) purified adult mouse DRG neurons *in vitro* reveal that GR is localized to neurons. NeuN is in green and DAPI in blue. Scale bar, 40 μm.

basis of micrograms loaded. For the hippocampus, 2 µg of protein was loaded for the β-actin blot, and 20 µg for the GR blot. For the DRG, 5 µg of protein was loaded for the β-actin and 1 µg for the GR blot; $N = 4$ per condition for each experiment.

Restraint stress protocol

We previously showed that placing mice into well-ventilated polypropylene tubes (2.8 × 9.7 cm) for 1 h elicits a transient, but significant increase in circulating corticosterone (cort; Alexander et al., 2009). This method of acute restraint stress was used throughout the experiments described in this manuscript. Nonstressed mice remained undisturbed in their home cages.

Drugs

For *in vivo* experiments, mifepristone (RU486; 50 mg/kg, Sigma, caltalog M8046), cort (1.5 mg/kg, Sigma, catalog C174), and dexamethasone (dex; 2 mg/kg, Sigma, catalog D1756) were prepared in a sterile peanut oil vehicle (veh) and then injected in a 0.1-ml volume 1 h before cell harvest. Cells were plated and kept in Neurobasal A media for 72 h. The dose of injected cort was previously determined to reproduce stress-induced plasma cort concentrations (Alexander et al., 2009). All drugs were prepared fresh daily and delivered via intraperitoneal injection.

In vitro DRG neuron experiments

Mouse DRG were harvested after 1 h of restraint (stress) or without (nonstressed; ns), as described previously (Gensel et al., 2009). Briefly, we dissected cervical, thoracic and lumbar DRG neurons from terminally anesthetized adult mice and incubated them in dispase 2 (5 U/ml; Roche) and collagenase type 2 (200 U/ml; Worthington) for 45-60 min at 37°C in HBSS (Mediatech), followed by DNase 1 type 2 (250 µg/ml; Sigma) treatment for 5 min. Next, DRG were triturated in 0.5 ml of HBSS media through fire-polished Pasteur pipettes and spun at 3000 rpm for 3 min. The neuron-enriched pellet was resuspended in 0.1 ml of Neurobasal A media supplemented with 2% B27, 1% Glutamax, and 1% penicillin-streptomycin. Neurons were plated onto coverslips at 400 cells/coverslip, or for high-density growth analysis at 10,000 cells/coverslip. Cells assessed using automated microscopy were plated into 12-well tissue culture plates. All coverslips and tissue culture plates were pre-coated with 0.1 mg/ml of poly-L-lysine (Sigma) and 10 µg/ml of laminin (Invitrogen). DRG neurons grew for 15, 24, or 72 h at 37°C in a 5% CO_2 humidified incubator. Different culture durations were used to interrogate different mechanisms of GC-GR-dependent growth (see Results). All DRG neurons were fixed with 2% paraformaldehyde (PFA) in PBS for subsequent immunohistochemistry. For each experiment, DRG neurons were prepared from three animals, and at least three coverslips or wells were used to quantify neurites using either Scholl Analysis or high-density neurite growth assays (below).

Rabbit polyclonal anti-β-tubulin III antibody (1:2000; Sigma, #T2200, RRID: AB_262133) or a combination of chicken anti-neurofilament (NF) 200 and 68-kDa antibodies [1:1000; Aves Labs, #NFL, NF heavy (NFH), RRID:

AB_2313553 and AB_2313552] were used to visualize DRG neurons and processes. Alexa Fluor 546-conjugated goat anti-rabbit or anti-chicken IgG secondary antibodies were paired with primary antibodies to detect DRG neurons (1:1000; Invitrogen). For high-density assays at least 45% of the coverslip was randomly sampled and digitized to quantify neurites (~100 fields; MCID 6.0 Elite). Using automatic densitometric threshold detection, neurons that were positively stained for β-tubulin III or NF were quantified then neurite density was normalized to total soma number in each field. Individual neuron neurite length in low-density cultures was quantified randomly on isolated DRG neurons after digitizing them on a light microscope followed by unbiased automated Sholl analysis (Gensel et al., 2011). Templates of concentric circles of 50-µm intervals were overlaid onto the center of a digitized DRG soma. For each neuron, densitometric thresholds were set to remove background labeling and clearly identify detailed cellular processes. The total number of objects above threshold intersecting each circle was tallied using an automated macro. The maximal ring with an intersecting process (max distance) and sum of the number of intersections (branching complexity or sprouting index) for all rings were generated for each cell and compared between groups. For automated analysis, at least 500 neurons in three technical replicates per experimental condition were examined, and each experiment was performed at least three times. In Figure 2*D-G*, individual DRG neurite length and branching were quantified using the Neuronal Profiling Algorithm (v4.1) on an ArrayScanXTI High Content Analysis Microscope (Thermo Fisher). At least 500 neurons per condition were analyzed.

Immunohistochemistry

Mice were anesthetized with 80 mg/kg of ketamine and 10 mg/kg of xylazine before transcardial perfusion with 30 ml 0.1 M PBS (pH 7.4) followed by 100 ml of 4% PFA in PBS. DRGs were embedded in optimal cutting temperature compound (OCT; Tissue-Tek, VWR International) and frozen at -80°C; 10- to 20-μm sections were cut using a cryostat and thaw-mounted on SuperFrost Plus slides (Fisher Scientific), then stored at -20°C until use. After drying at RT, slides were rinsed with 0.1 M PBS and overlaid with blocking solution for 1 h. Sections were subsequently washed and incubated overnight with the primary antibody and appropriate secondary antibodies. We used the following primary and secondary antibodies: GR: 1:200, #PA1-511A, Thermo Fisher, RRID: AB_2236340 or sc-8992, Santa Cruz Biotechnology, RRID: AB_2155784; SCG10, 1:500, Novus Biotechnologies anti-stathmin-2, NBP1-49467, RRID: AB_10011568; ATF3, 1:500, sc-188, Santa Cruz, RRID: AB_2258513; NFH, 1:1000; Aves Labs, RRID: AB_2313552; 555 or 488-conjugated goat anti-rabbit IgG antibody, 1:500 #A11035, Invitrogen. Hoechst or DAPI was applied in the final rinse to visualize nuclei.

Generation of samples for qPCR analysis

A 30-s sciatic nerve crush was performed as described below. In stress + injury groups, 1 h of restraint stress (see above) was performed before injury. L3-L5 DRGs ipsilateral to the injury were removed, trimmed of their axons and then placed into Trizol for RNA extraction. A total of 500 ng of RNA was used to prepare cDNA with the RT-for-PCR cDNA kit (Clontech), and qPCR was performed as described below.

qRT-PCR

Gene-specific primers were used for qRT-PCR to compare expression between ns and stress groups. All primers are listed 5'-3': *Ankrd1*: CAATGGGGCCGCAGGGGAAT, GCTTCACGCTGTTGGCCGGA; *Atf3*: AAGGGGTGATGCAA CGCGCT, CGCGGGTTAGCCGATTGGCT; *Jun*: GAGTGGGAAGGACGTGGCGC, TCCATCGTTCTG-GTCGCGCG; *Gap43*: GCCCCCTCCGAGGAAAAGGC, TG-GCTGGGCCATCTTCAGCC; *Il6*: GCCTTCTTGGGACTGAT-GCT,AGTCTCCTCTCCGGACTTGTG; *Sprr1a*: CCATTGCCTTGTGCTACCAA,TCAGGAGCCCTTGAAGAT-GAG; *Tp53*: AGCAGGGCTCACTCCAGCTACC,GGCTGGT-GATGGGGACGGGAT; *Stat3*: CGGCAGCCTGTCTGCA-GAGTT,ACCAGGCAATCACAATTGGCACG; *Tsc22d3*: bhCTCGAGGGGTCGACGGAGCC,AGGTGAGCG-GCACTCGGTCT; *Sgk*: GCCGGAGCGCACTGTTGTCTT,C-CGATGCCCGGAAAGAGCCC; *Cebpa*: GGTACG-GCGGGAACGCAACA, GAAGATGCCCCGCAGCGTGT; *Hspb2*: GGGCTCCAGTCCGGCACTTC,GCGGCGCTCG-GTCATGTTCT; *Cebpb*: CGCGTTCATGCACCGCCTGC, CCAGGCAGTCGGGCTCGTAGTAG; and *Hif1a*: TCTCG-GCGAAGCAAAGAGTCTG, CCCACACTGAGGTTGGT-TACTGTTG. Primer sequence specificity was confirmed by performing BLAST analysis for similar sequences against known sequence databases. PCRs were conducted in triplicate using 0.001 g of cDNA/reaction and Power SYBR Green master mix (Applied Biosystems) in 0.010-ml reactions. PCR product was measured using SYBR Green fluorescence on an Applied Biosystems 7900HT system. Standard curve and melting point analyses were performed to confirm amplification efficiency and single amplified products, respectively. The $\Delta\Delta$Ct analysis was used to normalize gene data to 18s ribosomal RNA reference gene expression. In all cases, expression was normalized to cDNA derived from L3-L5 DRGs from ns and noninjured mice; $N = 4$ mice per group.

Luciferase assays

The promoters of *Cebpa*, *Cebpb*, *Cebpd*, *Stat3*, *Hif1a*, *Il6*, and *Tp53* were amplified with promoter-specific primers which also contained restriction sites so that the promoter fragments (-1000 to +300 bp from the transcription start site) could be cloned into the pLightSwitch_Prom plasmid (SwitchGear Genomics) using the In-Fusion HD Cloning Kit (Clontech). The primers are show 5'-3': *Sgk1*: CTAGC-CCGGGCTCGAGTGAACGCTTACTGGTTTTGG, TTACT-TAGTTAAGCTTTGCGGCAGCGACTGCAGTAA; *Hspb2*: CTAGCCCGGGCTCGAGTGTTGATAAATTTGCATGTG, TACTTAGTTAAGCTTTTTGGACACGGAAGTCAATG; *Cebpa*: CTAGCCCGGGCTCGAGTCCCCGATT CAAGTTCACTC, TACTTAGTTAAGCTTCGTGCTCGCA-GATGCCGCCC; *Cebpb*: CTAGCCCGGGCTCGAGGT-CAATGGGTCGGGGGTCAG, TACTTAGTTAAGCT-TGGGCTGAAGTCGATGGCGCG; *Cebpd*: CTAGCCC GGGCTCGAGGGAGCTAGGCTGCTCTGTG, TTACTTAGT-TAAGCTTTGTTGAAGAGGTCGGCGAAG; *Stat3*: CTAGC-

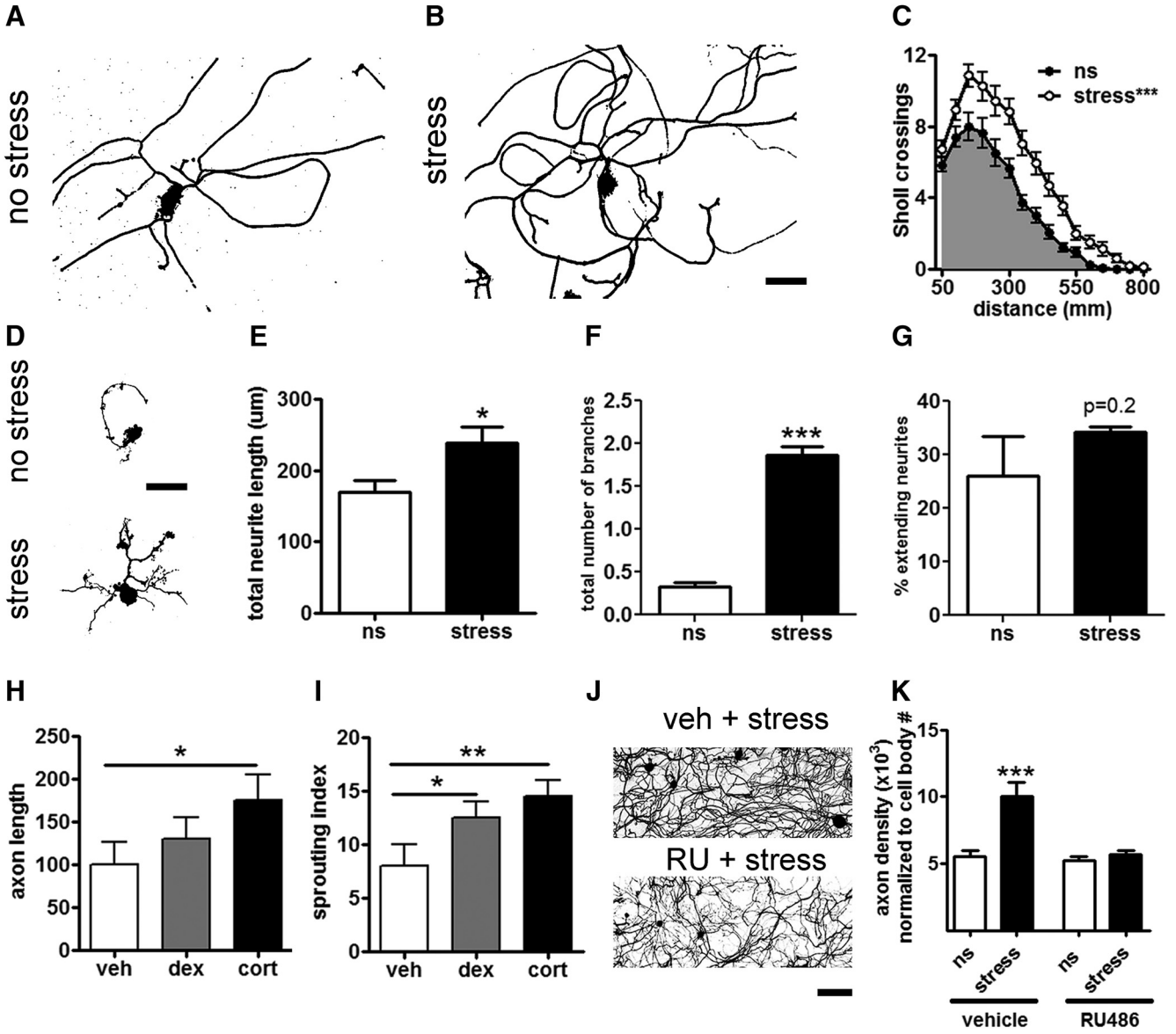

Figure 2. Acute stress promotes neurite growth via a GC-GR-dependent mechanism. ***A***, ***B***, DRG neurons were isolated from ns or stressed mice and grown *in vitro* for 72 h. Scale bar, 100 µm. ***C***, Stress increased neurite length. $***p < 0.0001$ versus ns, one-way ANOVA. ***D-F***, Stress increases neurite growth during the "arborizing" phase of DRG neurite outgrowth. ***D***, DRG neurons from Thy1-GFP-M transgenic mice were isolated from ns adult mice or adult mice subjected to 1 h of restraint stress and grown for 15 h *in vitro*. Scale bar, 100 µm. ***E***, ***F***, Stress increased neurite total length and the number of branches per neurite, $*p < 0.05$, $***p < 0.0001$, mean and SEM are shown. ***G***, The percentage of neurons extending neurites was unaffected by stress. All parameters were defined by the Neuronal Profiling Algorithm v4.1 (Cellomics ArrayScanXTI, Thermo Fisher). $N \geq 550$ neurons per condition. ***H***, ***I***, Cort administration (1.5 mg/kg) 1 h before DRG harvest increased neurite elongation and sprouting measures 24 h after plating *in vitro*. ***I***, The synthetic GC, dex (2 mg/kg) increased neurite sprouting, $*p < 0.05$, $**p < 0.01$. ***J***, Representative images of high-density DRG neuron cultures (72 h *in vitro*) from vehicle-treated and RU486-treated (RU) stressed mice. Scale bar, 200 µm. ***K***, The GR antagonist, RU486 blocked stress enhanced neurite growth, $***p < 0.0001$ versus ns, mean ± SEM are shown.

CCGGGCTCGAGGTTTTTCTGCACAAGGTGTG, TACTTAGTTAAGCTTCCTGCACCCCCTTCACCTGT; *Hif1a*: CTAGCCCGGGCTCGAGCACCAGCGGACCACAGGGCT, TACTTAGTTAAGCTTCGACTTTCTCAGGCAGAAAA; *Il6*: CTAGCCCGGGCTCGAGGAGGTCCTTCTTCGATATCT, TTACTTAGTTAAGCTTGAAGTCTCCTCTCCGGACTT; and *Tp53*: CTAGCCCGGGCTCGAGACACCTCAAGCGCTGGAGAA, TACTTAGTTAAGCTTGCCAAGCTTCCATTCCGCCC. All plasmids were validated by restriction digest and sequencing. The promoter containing plasmids were individually cotransfected with wtGR, constitutively active GR (caGR) (a truncated form of GR, missing the last 250 amino acids; Addgene; pG1-GR526; plasmid #1124) or EGFP into HEK293 cells grown in a 96-well format. All transfections were conducted according to the manufacturer's recommendations (Lipofectamine 2000, Invitrogen). HEK293 cells were cultured for 2 d *in vitro*, fluorescence was checked visually to confirm a successful transfection, and

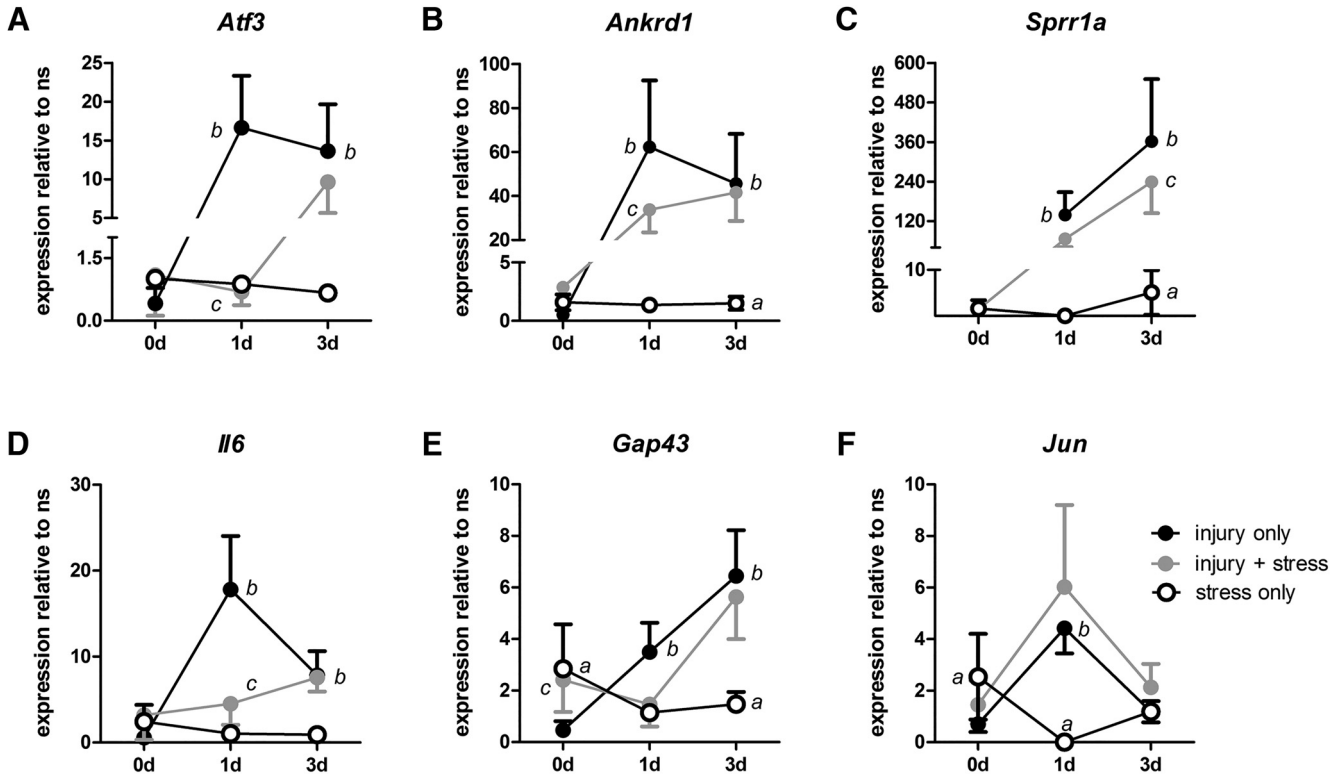

Figure 3. Stress represses injury-induced RAG expression. ***A-F***, RAG expression in DRGs was evaluated by qRT-PCR from ns mice and compared to expression in DRGs isolated immediately (0) or 1 or 3 d after: stress only (open circles), injury only (black circles), or when restraint stress was applied 1 h before injury (gray circles). Stress alone increases *Gap43* (***E***) and *Jun* (***F***) expression at 0 d, represses *Jun* at 1 d (***F***), and increases *Ankrd1* (***B***), *Sprr1a* (***C***), and *Gap43* (***E***) at 3 d. Stress compared to ns, $^{a}p < 0.05$-0.0005. ***A-F***, Injury significantly increases expression of all RAGs at 1 d and *Atf3* (***A***), *Ankrd1* (***B***), *Sprr1a* (***C***), *IL6* (***D***), and *Gap43* (***E***) at 3 d. Injury compared to ns mice, $^{b}p < 0.0001$. ***A***, ***B***, ***D***, Stress-reduced injury induction of *Atf3* (***A***), *Ankrd1* (***G***), and *Il6* (***I***) at 1 d; *Sprr1a* (***H***) at 3 d; and increased *Gap43* at 0 d. Injury compared to injury + stress, $^{c}p < 0.001$-0.0001, one-way ANOVA with Bonferroni or Fisher's *post hoc* tests. Mean ± SD are shown, $N = 4$ per group.

then the luciferase assay was performed following the manufacturer's recommendations (SwitchGear Genomics). For each experiment 8 replicate wells were transfected for each condition (e.g., promoter alone, promoter + wtGR, promoter + caGR) and the values attained from the luminometer were normalized to the average of the promoter only wells to generate a fold change value; $N = 8$ replicates per plate, $N = 3$ independent experiments.

Quantification of GR nuclear localization GR was visualized in DRG sections using an Axioplan 2 imaging microscope (Zeiss). All images were captured using identical exposure times, which were optimized for detecting GR in DRG from ns mice. Ganglia from L3-L5 were collected and imaged from three separate mice for each condition, and at least two sections were imaged from each ganglion. GR intensity was quantified in at least 50 randomly selected neurons using the Measure tool in ImageJ (Schneider et al., 2012). Neuron size was also measured and used to compare differences between small (10-26 µm), medium (27-42 µm) and large (43-58 µm) DRG neurons. Hoechst (Sigma) staining was used to visualize nuclei. The estimated ratio of cytoplasmic to nuclear GR intensity was calculated then these values were normalized to the average value in ns ganglia.

In vivo analysis of sciatic nerve regeneration Eight-week-old female C57BL/6 mice (Taconic) were anesthetized (80 mg/kg ketamine; 5 mg/kg xylazine) then, following shaving and aseptic preparation of the right hind leg, a Dumont #5 forceps was used to crush (30-s duration) the sciatic nerve. Stressed mice underwent 1 h of restraint just before injury. The site of nerve injury was marked by charcoal. This crush duration did not produce gross motor impairment (e.g., foot drop) postoperatively. The muscle/fascia layer was pulled together and the skin was sealed with a single wound clip (Stoelting). Three days after crush injury, mice were perfused, and sciatic nerves were harvested then prepared for histology as described above. Slides were incubated overnight at 4°C with the anti-SCG10 antibody. The next day, sections were washed then incubated for 1-2 h with Alexa Fluor 555- or 488-conjugated goat anti-rabbit IgG antibodies. Nerves were imaged with identical exposure times (Axioplan 2 imaging microscope, Zeiss). A photo montage was created in Photoshop then SCG10 intensity was quantified using ImageJ as described previously (Abe et al., 2010; Shin et al., 2012; Cho et al., 2013). Briefly, the width of each nerve was measured every 500 µm then averaged. The raw intensity every 100 µm was measured then normalized by dividing by average nerve width. The crush

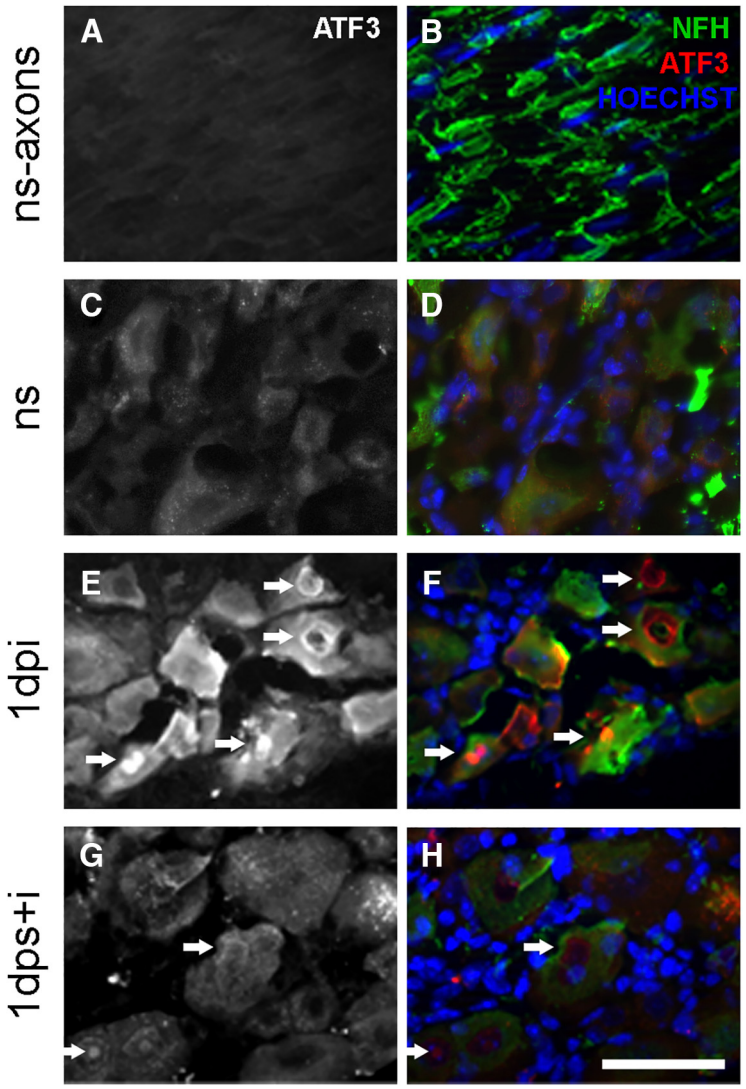

Figure 4. Stress reduces ATF3 immunostaining in DRG neurons. ***A***, ***B***, ATF3 was nearly undetectable in sensory neuron axons and (***C***, ***D***), DRG neurons from ns mice. ***E***, ***F***, DRG collected 1 dpi showed increased ATF3 immunoreactivity compared to DRGs collected from mice receiving stress + injury, ***G***, ***H***, Arrowheads indicate ATF3 nuclear immunoreactivity. ***B***, ***D***, ***F***, ***H***, NFH is shown in green, ATF3 in red, and Hoechst in blue. Scale bar, 100 µm.

site was identified as the point with the highest intensity as in (Shin et al., 2014) . The regeneration index was calculated as the farthest point from the site of injury where pixel intensity was at least 50% of the intensity at the crush site (Abe et al., 2010); $N = 4$ nerves/mouse; $N = 3$ mice/group.

A separate cohort of mice was used for 3-dimensional (3D) imaging and axon quantification. The same 30-s unilateral sciatic nerve crush injury was performed on eight-week-old female Thy1-GFP-M (The Jackson Laboratory, stock #007788) mice (Feng et al., 2000). These mice were perfused at 14 d postinjury (dpi). After perfusion, sciatic nerves were rapidly removed and postfixed overnight at 4°C, followed by a rinse in 100 mM PBS. Sciatic nerves were cleared using 50% tetrahydrofuran (THF) for 25 min, 80% THF for 30 min, 100% THF 2Xs for 30 min, 100% dichloromethane for 20 min, and finally in Dibenzyl ether (Sigma-Aldrich) for 15 min (Ertürk et al., 2012). The whole sciatic nerve was imaged using a fluorescence light sheet microscope (LaVision BioTec Ultramicroscope). Axon quantification was performed with an unbiased approach, using the Spots algorithm in Bitplane Imaris Scientific 3D/4D Image Processing Software (Oxford Instruments) at 0.5-mm intervals from the crush site to the distal end of the nerve. The number of "spots" at each interval was entered for each mouse ($N = 3$/group) then compared between groups (stress vs no-stress).

Statistics *In vitro* and *in vivo* neurite/axon growth was analyzed using one- or two-way repeated measures analysis of variance with Bonferroni or Fisher *post hoc* analyses. Student's *t* test was used to analyze data from histologic experiments comprising only two groups. A ratio *t* test for paired data were applied to Western blot analyses to compare fold change between groups. An α-level of $p < 0.05$ was used to indicate statistical significance.

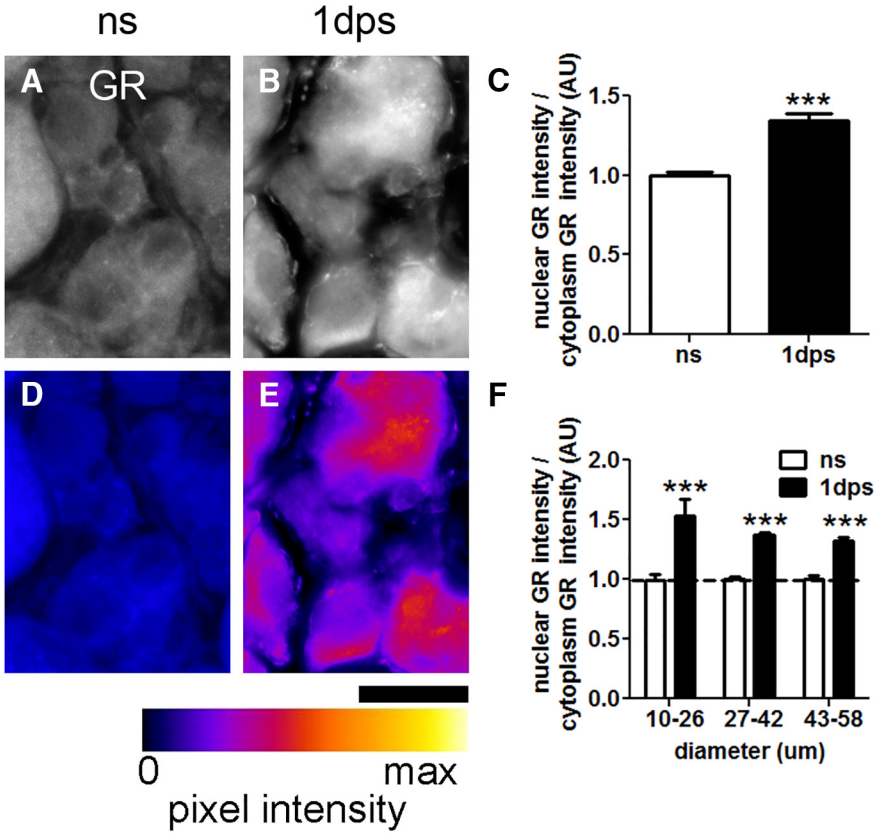

Figure 5. Stress increases GR nuclear localization in DRG neurons. ***A***, ***B***, GR immunofluorescence in DRG neurons from ns and stressed (1 d ps) mice. ***D***, ***E***, Images in ***A***, ***B*** converted to an intensity map overlay using the Fire lookup table (ImageJ). Fire LUT pixel intensity map key show colors corresponding to pixels from 0 to max intensity. Scale bar, 25 µm. ***C***, Stress increases nuclear GR pixel intensity in DRG compared to ns mice. $N \geq 50$ neurons (see Materials and Methods). One-way ANOVA followed by Bonferroni *post hoc* tests, compared to ns. Mean and SEM are shown, $***p < 0.0001$. ***F***, Cell areas were divided into three groups to represent small (10-26 µm), medium (27-42 µm), and large (43-58 µm) DRG neurons. Increases in GR nuclear localization were consistent across different sized DRG neurons.

Results

Sensory neurons express high levels of GRs

Stress activates the hypothalamic-pituitary-adrenal axis leading to an increase in the synthesis and release of GCs into the circulation. High levels of circulating GCs directly regulate gene transcription by binding to GRs. Hippocampal neurons express high levels of GRs, and GC-GR interactions profoundly affect hippocampal neuron structure/function (Sapolsky et al., 1984; Joëls et al., 2003; Fitzsimons et al., 2013). In sensory neurons, however, neither the relative abundance of GRs nor the effects of GC-GR interactions are known. We used Western blotting to compare the relative amounts of GRs in spinal cord, hippocampus, DRG and cortex. Although GRs were found in all regions, GR levels in DRG were ~15-fold greater than in the hippocampus (Fig. 1*A*,*B*). Whole DRGs or purified adult DRG neurons labeled with anti-GR antibodies confirmed GR localization predominantly in neurons (Fig. 1*C*,*D*). These data indicate that DRG neurons express surprisingly high levels of GRs, suggesting that circulating or exogenous GCs may exert potent effects on DRG neurons through GRs.

Stress induces sensory neurite growth

Stress and GCs induce structural plasticity in hippocampal neurons with corresponding behavioral changes that manifest as impaired cognition and anxiety. Previously, we found that stress and GCs enhance nerve injury-induced pain (Alexander et al., 2009). To test whether the enhanced nociceptive effects of stress and GCs were also associated with structural changes in sensory neurons, adult DRG neurons were isolated from stressed or ns mice, then morphologic features of neurite growth were analyzed. Immediately after stress, DRG neurons were isolated and placed in culture for 72 h, a time in which most DRG neurons have extended neurites. Neurite length and complexity were analyzed using unbiased automated Sholl analysis (Gensel et al., 2011). Stress consistently and significantly increased the complexity (number of Sholl crossings; indicative of arborization) and overall length of neurites *in vitro* (Fig. 2*A-C*).

Stress promotes neurite growth via GC-GR-dependent regulation of genes that are constitutively expressed in sensory neurons

Previous data indicate that neurite outgrowth from uninjured adult DRG occurs in two phases (Smith and

Skene, 1997). In the early phase (~12-16 h after plating), small numbers of neurons exhibit highly branched arborizing neurites but limited extension of any individual neurite. Genes that are constitutively expressed *in vivo* by DRG neurons regulate this early (arborizing) phase of neurite growth. In the second phase (≥24 h), most DRG neurons develop the capacity for rapid and sustained axonal elongation. This later and distinct phase of axon growth requires transcription of new genes including various canonical RAGs (e.g., GAP43; Smith and Skene, 1997; Frey et al., 2000; Cafferty et al., 2001; Bonilla et al., 2002; Campbell et al., 2005; Qiu et al., 2005; Seijffers et al., 2007).

Because data in Figure 2*A-C* were generated from DRG neurons cultured for 72 h, it is not possible to know whether stress affected the constitutively expressed genes that control early neurite growth or the later RAG-dependent growth programs. Thus, in a follow-up experiment, DRG neurons were isolated from ns or stressed mice, then grown in culture for 15 h, a time preceding the delayed induction of RAG expression (Smith and Skene, 1997). After 15 h, neurons from ns mice extended short neurites (<200 µm) with few arborizations (Fig. 2*D*). In contrast, stress increased the overall length and branching complexity of DRG neurites (Fig. 2*E*,*F*); the total number of DRG neurons with multibranched neurites tripled, and the total number of branches/neuron increased 6-fold. Stress did not affect the percentage of neurons that extended neurites (Fig. 2*G*), indicating that stress acts on existing neurite outgrowth pathways to induce neurons to extend neurites at a faster rate.

To determine if these acute effects of stress could be mediated by GCs, in lieu of stress, naïve mice were injected intraperitoneally with cort (1.5 mg/kg) or a synthetic GC (dex; 2 mg/kg) 1 h before DRG harvest. Neurons were evaluated at 24 h, well before the marked increases in RAG expression that occurs in cultured DRG neurons (Smith and Skene, 1997). Structural plasticity increases similar to those caused by stress were seen with either cort or dex; cort increased neurite length and complexity, whereas dex increased only neurite sprouting (Fig. 2*H*,*I*).

To determine if the stress/GC effects were mediated via binding to GR *in vivo*, mice were injected with the GR-antagonist RU486 (50 mg/kg) before stress. High-density DRG neuron cultures were used since they require less effort to prepare and analyze, and because stress and cort were found to increase the density of neurites in high-density cultures (data not shown). As shown in Figure 2*J*,*K*, acute GR block with RU486 prevented the increase in neurite outgrowth caused by stress.

Combined, these data indicate that stress enhances axon outgrowth from sensory neurons in part via GC-GR-dependent interactions. These changes occur early (<24 h), before axotomy induced transcriptional programs, and thus might work through GC-GR-dependent transcription pathways.

Stress promotes DRG neurite growth independently of RAGs

The ability of stress to induce vigorous neurite growth in DRG neurons is reminiscent of the "conditioning effects" of a peripheral nerve injury. Indeed, DRG neurons that have been previously injured have an increased ability to initiate regenerative axon growth and this is dependent on new gene transcription (i.e., RAGs; Smith and Skene, 1997; Frey et al., 2000; Cafferty et al., 2001; Bonilla et al., 2002; Campbell et al., 2005; Qiu et al., 2005; Seijffers et al., 2007). To test whether expression of canonical RAGs that are normally induced by nerve injury (e.g., *Atf3*, *Ankrd1*, *Sprr1a*, *Il-6*, *Gap43*, and *Jun*) also are upregulated by stress, mRNA was prepared from DRG neurons that were isolated from mice immediately following stress (0 d), or 1 or 3 d after exposing them to 1 h of restraint stress (Fig. 3*A-F*, open circles). Stress increased the expression of *Ankrd1*, *Sprr1a*, *Gap43*, and *Jun* mRNA; however, the magnitude and temporal progression of these changes varied by gene. Both *Gap43* and *Jun* mRNA were immediately increased (relative to ns mice, 0 d; Fig. 3*E*,*F*, open circles). Conversely, *Ankrd1* and *Sprr1a* increased but not until 3 d after stress. Although *Jun* expression increased immediately after stress, *Jun* expression was significantly reduced by 1 d (relative to ns), a finding consistent with GR-dependent regulation of *Jun* (Wei et al., 1998). *Jun* expression returned to baseline by 3 d (Fig. 3*F*). Overall, stress had only a mild effect on inducing expression of a subset of RAGs. By comparison, RAG

Table 1. TFs associated with regeneration whose expression is also impacted by the GR (transcriptionally activated/repressed by GR)

Transcription factor	Effect of GR on transcription
C/EBPα	+
C/EBPβ	+
COUP-TFII	+
c-Rel (NF-κB subunit)	+
HIF1A	+
IRF1	+
NURR1	+
p73	+
PPAR-γ	+
SF1	+
STAT3	+
STAT5	+
STAT5A	+
STAT5B	+
TBP	+
c-Jun/c-Fos	-
c-Rel (NF-κB subunit)	-
E2A	-
NF-AT2(NFATC1)	-
NF-κB	-
NF-κB1 (p50)	-
p53	-
p73	-
PIT1	-
RelA (p65 NF-κB subunit)	-
SMAD3	-
STAT6	-
T-bet	-
ZNF307	-

Interactions were determined using MetaCore software and were identified in mouse, rat, and human.

Table 2. GR regulated TFs in column A (interaction from) and the targeted downstream RAGS in column B (interaction to)

Interaction from	Interaction to	Interaction effect	Interaction type	Organisms
c-Rel (NF-κB subunit)	c-Myb	+	TR	Homo;Mus;Rattus
c-Rel (NF-κB subunit)	STAT1	u	TR	Homo;Mus;Rattus
c-Rel (NF-κB subunit)	STAT5A	u	TR	Homo;Mus;Rattus
c-Rel (NF-κB subunit)	IL-6	+	TR	Homo;Mus;Rattus
C/EBPα	RNF12	u	TR	Homo;Mus;Rattus
C/EBPα	c-Fos	+	TR	Homo;Mus;Rattus
C/EBPβ	STAT6	+	B	Homo;Mus;Rattus
C/EBPβ	b-Myb	u	TR	Homo;Mus;Rattus
C/EBPβ	LTBP2	u	TR	Homo;Mus;Rattus
C/EBPβ	HNF1-α	+	B	Homo;Mus;Rattus
C/EBPβ	HNF1-β	+	B	Homo;Mus;Rattus
C/EBPβ	PAX2	u	TR	Homo;Mus;Rattus
C/EBPβ	c-Jun	+	B	Homo;Mus;Rattus
C/EBPβ	Ghrelin	u	TR	Homo;Mus;Rattus
C/EBPβ	IL-6	+	TR	Homo;Mus;Rattus
C/EBPβ	c-Fos	+	TR	Homo;Mus;Rattus
c-Jun/c-Fos	c-Fos	u	TR	Homo;Mus;Rattus
COUP-TFII	HNF1-β	+	TR	Homo;Mus;Rattus
E2A	ZNF143	u	TR	Homo;Mus;Rattus
E2A	c-Fos	u	TR	Homo;Mus;Rattus
GCR-α	STAT5A	+	B	Homo;Mus;Rattus
GCR-α	TBP	+	B	Homo;Mus;Rattus
GCR-α	STAT6	-	B	Homo;Mus;Rattus
GCR-α	c-Jun/c-Fos	-	B	Homo;Mus;Rattus
GCR-α	SMAD3	-	B	Homo;Mus;Rattus
GCR-α	IL-6	-	TR	Homo;Mus;Rattus
GCR-α	ZNF167	u	TR	Homo;Mus;Rattus
HIF1A	IL-6	+	TR	Homo;Mus;Rattus
HIF1A	SMAD3	+	B	Homo;Mus;Rattus
HIF1A	Mxi1	+	TR	Homo;Mus;Rattus
HIF1A	RNF183	u	TR	Homo;Mus;Rattus
HIF1A	c-Jun	+	B	Homo;Mus;Rattus
HIF1A	Junctin	+	TR	Homo;Mus;Rattus
IRF1	RNF168	u	TR	Homo;Mus
IRF1	c-Myb	-	TR	Homo;Mus;Rattus
IRF1	RNF12	u	TR	Homo;Mus;Rattus
IRF1	c-Jun	+	B	Homo;Mus;Rattus
NF-AT2(NFATC1)	LTBP3	+	TR	Homo;Mus;Rattus
NF-κB	PAX2	u	TR	Homo;Mus;Rattus
NF-κB	PTBP1	u	TR	Homo;Mus;Rattus
NF-κB	FosB	u	TR	Homo;Mus;Rattus
NF-κB	JunB	u	TR	Homo;Mus;Rattus
NF-κB	Ghrelin	u	TR	Homo;Mus;Rattus
NF-κB	Junctin	u	TR	Homo;Mus;Rattus
NF-κB	STAT5A	u	TR	Homo;Mus;Rattus
NF-κB	IL-6	+	TR	Homo;Mus;Rattus
NF-κB	SMAD3	+	B	Homo;Mus;Rattus
NF-κB1 (p50)	c-Fos	-	B	Homo;Mus;Rattus
NF-κB1 (p50)	c-Myb	+	TR	Homo;Mus;Rattus
NF-κB1 (p50)	JunB	u	TR	Homo;Mus;Rattus
NF-κB1 (p50)	IL-6	+	TR	Homo;Mus;Rattus
NF-κB1 (p50)	FosB	u	TR	Homo;Mus;Rattus
NF-κB1 (p50)	c-Jun	-	B	Homo;Mus;Rattus
Oct1	JunD	u	TR	Homo;Mus;Rattus
Oct1	IL-6	u	TR	Homo;Mus;Rattus
Oct1	FosB	u	TR	Homo;Mus;Rattus
Oct1	STAT4	u	TR	Homo;Mus;Rattus
Oct1	LTBP3	u	TR	Homo;Mus;Rattus
Oct1	HNF1-β	u	TR	Homo;Mus;Rattus
Oct1	HNF1-α	+	B	Homo;Mus;Rattus
p53	RNF10	u	TR	Homo;Mus;Rattus

(Continued)

Table 2. Continued

Interaction from	Interaction to	Interaction effect	Interaction type	Organisms
p53	STAT4	u	TR	Homo;Mus;Rattus
p53	b-Myb	-	B	Homo;Mus;Rattus
p53	TBP	-	B	Homo;Mus;Rattus
p53	A-Myb	u	TR	Homo;Mus;Rattus
p53	c-Myb	-	B	Homo;Mus;Rattus
p53	Large T antigen (SV40)	+	B	Homo;Mus;Rattus
p53	STAT5A	-	Unspecified	Homo;Mus;Rattus
p53	c-Fos	u	TR	Homo;Mus;Rattus
p53	IL-6	-	TR	Homo;Mus;Rattus
p73	ZNF143	+	B	Homo;Mus;Rattus
p73	STAT1	+	TR	Homo;Mus;Rattus
PIT1	c-Fos	+	TR	Homo;Mus;Rattus
PPAR-γ	SMAD3	-	B	Homo;Mus;Rattus
RelA (p65 NF-κB subunit)	STAT6	u	TR	Homo;Mus;Rattus
RelA (p65 NF-κB subunit)	RhoA	+	TR	Homo;Mus;Rattus
RelA (p65 NF-κB subunit)	JunB	+	TR	Homo;Mus;Rattus
RelA (p65 NF-κB subunit)	STAT5A	+	TR	Homo;Mus;Rattus
RelA (p65 NF-κB subunit)	FosB	+	TR	Homo;Mus;Rattus
RelA (p65 NF-κB subunit)	IL-6	+	TR	Homo;Mus;Rattus
RelA (p65 NF-κB subunit)	ZNF143	u	TR	Homo;Mus;Rattus
SMAD3	c-Jun	+	TR	Homo;Mus;Rattus
SMAD3	LTBP3	+	TR	Homo;Mus;Rattus
SMAD3	JunB	+	TR	Homo;Mus;Rattus
SMAD3	c-Jun/c-Fos	+	B	Homo;Mus;Rattus
STAT3	ZNF148	-	B	Homo;Mus;Rattus
STAT3	STAT1	u	TR	Homo;Mus;Rattus
STAT3	IL-6	+	TR	Homo;Mus;Rattus
STAT3	JunB	+	TR	Homo;Mus;Rattus
STAT3	LTBP3	u	TR	Homo;Mus;Rattus
STAT3	STAT2	u	TR	Homo;Mus;Rattus
STAT3	c-Fos	+	TR	Homo;Mus;Rattus
STAT5	c-Fos	+	TR	Homo;Mus;Rattus
STAT5	STAT1	-	C	Homo;Mus;Rattus
STAT5A	c-Fos	+	TR	Homo;Mus;Rattus
STAT5B	STAT1	-	C	Homo;Mus;Rattus
STAT6	STAT1	-	C	Homo;Mus;Rattus
STAT6	RhoA	+	TR	Homo;Mus;Rattus
T-bet	STAT1	+	TR	Homo;Mus;Rattus
T-bet	SETBP1	+	TR	Homo;Mus;Rattus

The effect of the interaction on target gene expression is shown in column C, and the type of interaction is in column D. The organism this interaction was reported in is listed in column E. + indicates activation; - indicates inhibition; u indicates unspecified interaction. TR indicates transcription regulation; B indicates binding; C indicates competition. Homo: *Home sapiens*, Mus: *Mus musculus*; Rattus: *Rattus norvegicus*.

expression was markedly increased 1 and 3 d after a peripheral nerve injury in ns mice (Fig. 3*A-F*, black circles).

These data indicate that stress increases neuronal expression of a subset of RAGs, but that these effects are delayed and are orders of magnitude lower than the effects of a peripheral nerve injury. Thus, GR-dependent induction of canonical RAGs alone is unlikely to explain the consistent and substantial increase in neurite growth caused by stress (Fig. 2). In fact, based on timing and the relative magnitude of changes in RAG expression, stress/GCs and nerve injury appear to regulate neurite growth via independent transcriptional mechanisms.

To test this hypothesis, acute stress was applied for 1 h before a sciatic nerve crush. One or three days later, DRGs were dissected and gene expression was analyzed using qPCR. Using this approach, gene expression changes caused by stress and injury will occur together and interact in DRG neurons *in vivo*. Remarkably, restraint stress (1 h) before nerve injury caused a partial or complete block of the injury-induced increase in RAG expression (Fig. 3*A-F*, gray circles). Only nerve injury-induced changes in Jun expression were unaffected by stress (Fig. 3*F*). When compared to the effects of injury alone, stress significantly reduced the expression of most injury-induced RAGs; *Atf3*, *Ankrd1*, and *Il6* levels were significantly reduced in DRG neurons from stressed mice as compared to injury only mice (Fig. 3*A*,*B*,*D*, compare gray circles with black circles, *C*).

The effects of stress on reducing nerve injury-induced gene expression were most prominent for *Atf3*, with near complete inhibition of *Atf3* upregulation at 1 dpi (Fig. 3*A*). To determine if reduced *Atf3* expression was matched with a reduction in ATF3 protein, anti-ATF3 antibodies were used to label sections of DRG (Fig. 4). No ATF3 was detected in axons or neuronal somata from uninjured ns mice (Fig. 4*A-D*). As expected, nerve injury increased

Table 3. GR (*Nr3c1*) TF binding sites predicted by the JASPAR database (Wasserman and Sandelin, 2004)

Gene	Chromosome	Strand	Number of sites	Relative score	Position in promoter	Predicted binding site sequence
Ankrd1	19	-	2	0.8	723	CAAAGCAACACTTCCCAG
				0.82	738	AGAAATAGGATGTCCCAA
Atf3	1	-	3	0.75	731	GAAGGCACATTTTCCTGA
				0.75	1022	AAAAACGTTTTGTGGTTG
				0.8	1163	GAGATCAAAGCGTCCTCT
Cebp-α	7	+	3	0.77	216	AAAAAGAAAGTTTTCCAG
				0.75	336	GGGACCCTGTAGTTCTAG
				0.75	412	GAGAAAAAGACGCACAAT
Cebp-β	2	+	0			
Cebp-δ	16	+	2	0.75	102	GGACAGATGATTTTCTTG
				0.76	348	AGAAACAGCAAGATGCTA
Gap43	16	-	3	0.76	29	GAAAAAAAAATTTTTTTT
				0.75	381	AGAGAGAGAATGTGCGTG
				0.75	1209	AGAAAGAATCACAACTGT
Hif1a	12	+	3	0.75	672	CAGTTCCTCATGTCGTGG
				0.77	758	AAAATCATAATGTAAATA
				0.76	879	AAAAAAAAAACTTACGTG
Hsbp1(Hsp27)	9	+	2	0.75	600	CAAAACACTCACTCCAGA
				0.87	655	AAGAAAATTTTTTCCTAA
IL-6	5	+	1	0.84	352	AGAAACAACTGGTCCTGA
Jun	4	-	5	0.75	331	GGTGACATCATGGGCTAT
				0.79	419	CAGAGAAGAATCTTCTAG
				0.79	841	CAGATCATTCAGCCCTTT
				0.77	1003	CGAAACTAAACTTCCAAG
				0.77	1101	GAGAATAAAGTGTTGTGC
NFκBia	12	-	1	0.81	349	AGGACGAGCCAGTTCTTT
p21(Cdkn1a)	17	+	6	0.77	131	GACAGCATCCTTTCCTTC
				0.81	184	GAAATGATCGCGTTCTGG
				0.83	233	GGGAAAAAAATCTCCAGA
				0.77	616	AGGCAAACACTGTACCAA
				0.81	685	GAAAAGAGTTAGTCCTTC
				0.75	740	CAGCTCTAACTGTACTGT
p53	11	+	1	0.85	403	GAAAACAGTCTTTACAGA
Sgk1	10	+	3	0.76	579	GAGACCATTCACTGCTAC
				0.77	605	AGGCACATTATTTTATTT
				0.75	766	AAGAAAAACCAATTCAAA
Sprr1a	3	-	0			
Stat3	11	-	2	0.79	987	GGAAATGGCAAGTACTGT
				0.76	1069	GGAAACAAGTTGGTCAAA

For each gene, the promoter was defined as -1000 and +300 bp from the transcription start site.

somal ATF3 at 1 dpi (Fig. 4*E*,*F*). In contrast, minimal ATF3 was evident in DRG tissue sections from injured mice that had been stressed before nerve injury (Fig. 4*G*,*H*, arrowheads).

Together, data in Figures 2-4 indicate that stress increases neurite growth in a GC-GR-dependent manner; however, these effects occur without inducing the expression of canonical RAGs. In fact, stress blocks or suppresses the expression of RAGs that are normally increased by nerve injury.

Stress increases nuclear translocation of the GR

A stress-induced change in gene transcription should be associated with translocation of GR from the cytoplasm to the nucleus. To determine if this occurs in stressed DRG neurons, mice were subjected to acute stress for 1 h then 1 d later, DRGs were removed and stained with antibodies that label GR (Fig. 5*A*-*E*). In naive mice, GR labeling intensity was low (blue coloring; also see Materials and Methods; Fig. 5*A*-*D*). In contrast, stress markedly increased the ratio of nuclear to cytoplasmic GR intensity. These data indicate that stress promotes nuclear translocation of GR, and supports the notion that axon growth programs are affected by GR-dependent regulation of gene transcription.

Because phenotypically and functionally distinct classes of sensory neurons exist within DRGs (Usoskin et al., 2015; Li et al., 2015), stress or GCs may not uniformly affect nuclear translocation of GRs in these varied DRG neuron subtypes. To test this hypothesis, the mean GR signal intensities in Figure 5*C* were binned as a function of neuron diameter [e.g., small (10-26 µm), medium (27-42 µm), or large (43-58 µm)], a classification scheme that roughly correlates with division of DRG subtype by Trk family receptor expression (i.e., TrkA are small, TrkB are medium, TrkC are large diameter; McMahon et al., 1994; Usoskin et al., 2015). As shown in Figure 5*F*, GR nuclear intensity increased across all neuronal size classes, suggesting that GC/GR-dependent changes in gene expression affect all sensory neurons.

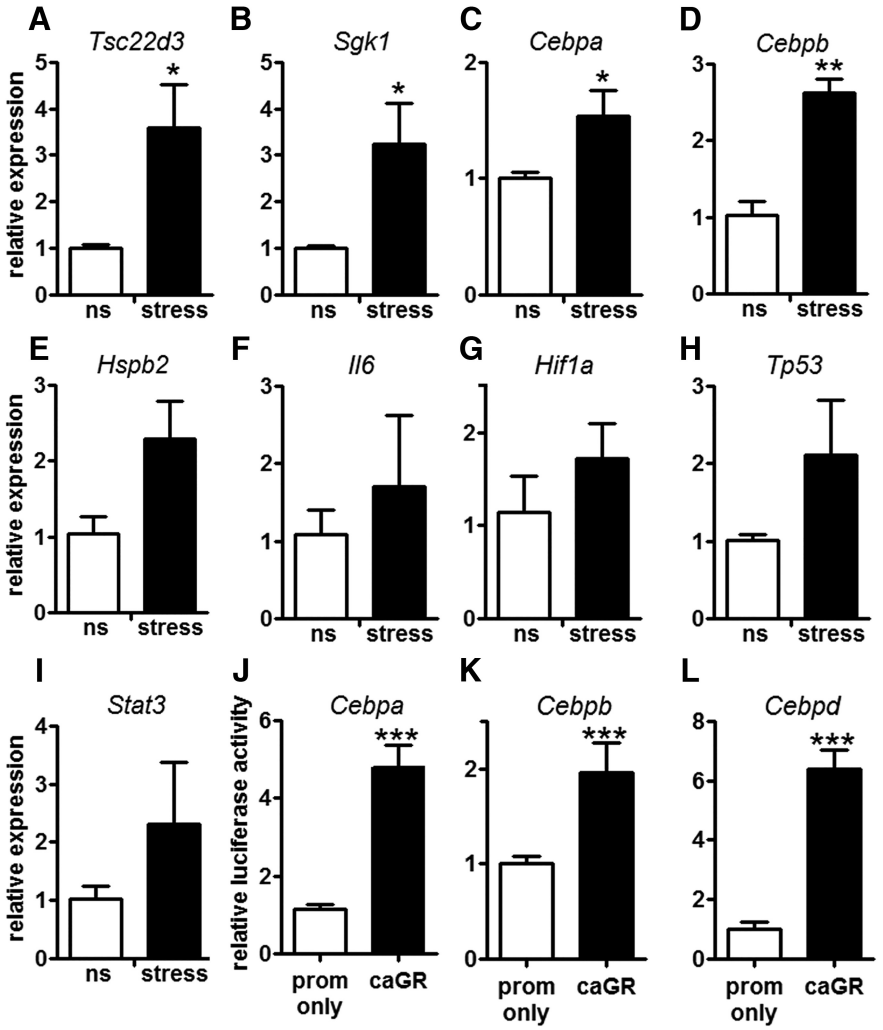

Figure 6. Stress and GRs activate *Cebp* TF expression. ***A-D***, Stress (1 h) increases *Tsc22d3* (***A***), *Sgk1* (***B***), *Cebpa* (***C***), and *Cebpb* (***D***) expression in DRG. *Hspb2* (***E***), *Il6* (***F***), *Hif1a* (***G***), *Tp53* (***H***), and *Stat3* (***I***) expression were unaffected; $N = 3$. ***J-L***, caGR increased luciferase expression from the *Cebpa* (***J***), *Cebpb* (***K***), and *Cebpd* (***L***) promoter; $N = 8$ replicates for each condition per experiment; $N = 3$ experiments. $***p < 0.0005$, one-way ANOVA followed by Dunnett's multiple comparison test with the promoter only as the control. Mean and SEM are shown.

Predicted transcriptional regulation of RAGs by the GR

To identify genes in sensory neurons that are directly activated or repressed by GRs, we first used GeneGo to analyze a list of >400 genes that had already been identified in injured DRG neurons (Seijffers et al., 2007; Stam et al., 2007; Hajji et al., 2008; Wu et al., 2008; Moore et al., 2009; Michaelevski et al., 2010). Using this approach, 28 transcription factors (TFs) were identified whose expression is directly increased or decreased by GR transcriptional activity or binding (Table 1). Next, we evaluated the list of >400 genes to identify genes regulated by these TFs. This approach identified an additional 100 genes (Table 2). In addition to known targets, several potentially novel GR targets were identified by scanning the putative promoter regions (-1000 bp, +300 bp from the transcription start site) of genes for predicted GR-response elements (GREs), i.e., short sequences bound by GRs (http://jaspar.genereg.net). GREs were identified in the promoters of several TFs and RAGs expressed in DRG neurons (Table 3), suggesting that GRs can exert a surprisingly large and diverse effect on the transcriptional machinery that controls sensory neuron growth and function.

To validate the *in silico* analysis above, qPCR was used to quantify a subset of genes/TFs in DRG neurons from control (ns) or stressed mice. Expression of *Tsc22d3* (also known as Gilz), a stress-induced gene with GREs in its promoter region, was analyzed as a positive control gene (Fig. 6*A*; Riccardi et al., 2000). Stress increased the expression of *Tsc22d3* and also *Sgk*, *Cebpa*, and *Cebpb* (Fig. 6*A-D*). Other RAGs, many of which have been described as potent transcriptional regulators of axon regeneration including *Hspb2* (also known as Hsp27), *Il-6*, *Hif1a*, *Tp53* (also known as p53), and *Stat3*, were also affected by stress, although gene expression changes were highly variable and were not significantly different from controls (Fig. 6*E-I*).

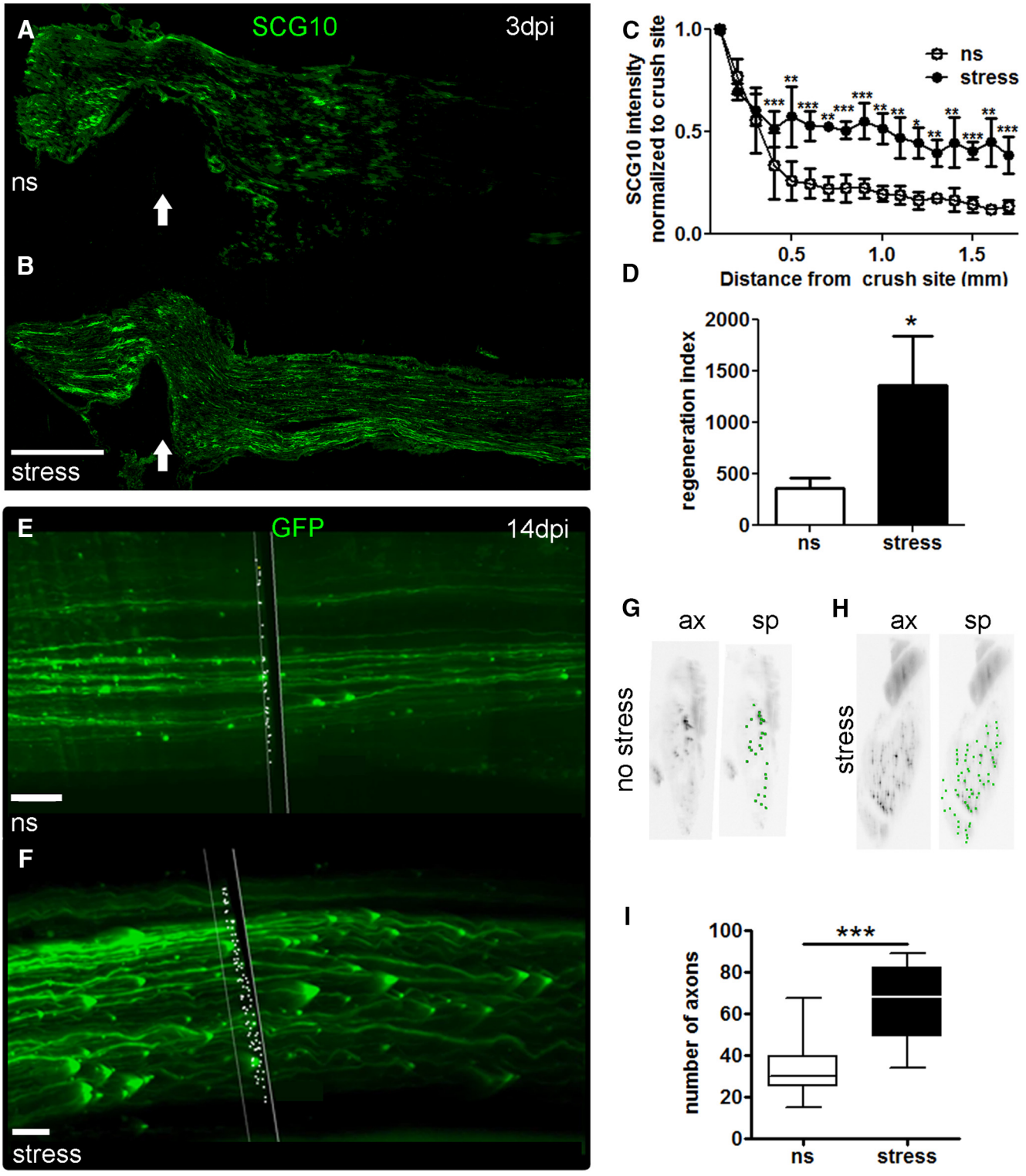

Figure 7. Stress enhances regeneration of injured sensory axons *in vivo*. ***A***, ***B***, Representative longitudinal sections of sciatic nerves from mice that received a crush injury alone or 1 h of restraint followed by crush injury. Nerves were immunostained with SCG10. Arrow indicates crush site. Scale bar, 500 µm. ***C***, Stress increased SCG10+ intensity distal to the crush site by 3 dpi. Results are expressed as mean ± SEM. $^{**}p < 0.001$, $^{***}p < 0.0001$ for two-way ANOVA for distance and condition; $N = 3$ per group, four sections per animal. ***D***, Stress increases the regeneration index. Results are expressed as mean ± SD. $^{*}p < 0.01$, unpaired *t* test. ***E-I***, Representative images of cleared intact sciatic nerve distal to the crush site in ns (***E***) and stressed (***F***) mice. The plane through the nerve (black box with white outline) and the white dots show the results of the Spots algorithm (Bitplane) used for axon quantification. Scale bar, 70 µm. ***G***, ***H***, A single cross section view through the intact sciatic nerve rendered in black and white for easy viewing (left panel; axons: ax). Green dots indicate axon cross sections and show the outcome of the spots algorithm (sp). ***I***, Summary

continued

statistics for the experiment are shown in a box plot for the average number of axons measured every 0.5 mm distal to the crush site in the sciatic nerve in ns and stressed mice. Average, 33 ns versus 64 stressed, $***p < 0.0001$; minimum, 15 ns versus 34 stressed; median, 30 ns versus 63 stressed; maximum, 68 ns versus 89 stressed; $N = 3$ per group.

To show that GC-GR interactions could play a role in inducing expression of these genes, we tested the ability of caGR to drive luciferase expression from the promoters of *Cebpa*, *Cebpb*, *Cebpd*, *Stat3*, *Hif1a*, *Sgk1*, *Hspb2*, *Il-6*, and *Tp53.* Luciferase activity was not changed when *Hif1a*, *Sgk1*, *Hspb2*, or *Tp53* were coexpressed with caGR and inconsistent luciferase activity was observed for *Stat3* and *Il-6* (data not shown). In contrast, transfection with caGR consistently increased luciferase activity from the promoters of *Cebpa*, *Cebpb*, and *Cebpd* (Fig. 6*J-L*). These data indicate that GR can bind to the promoters of *Cebpa* and *Cebpd* (Table 3), presumably through the predicted GREs, and that GRs can activate transcription of these genes.

Stress increases peripheral nerve axon regeneration

The experiments above indicate that stress increases sensory axon growth via GC-GR-dependent mechanisms. To determine if stress/GCs cause similar effects on axon growth *in vivo*, peripheral nerve regeneration was evaluated in ns and stressed mice that received a sciatic nerve crush. Sections of injured sciatic nerves (3 dpi) from stressed or ns mice were labeled with SCG10, a protein that is preferentially expressed in regenerating sensory axons (Shin et al., 2014). SCG10 intensity was significantly higher compared to ns mice (Fig. 7*A-C*). Also, the axon regeneration index, the point along the nerve at which the SCG10 labeling was half the intensity found at the crush site (Abe et al., 2010), was increased by stress (Fig. 7*D*).

To eliminate any variability or unintended sampling bias that might be associated with immunostaining or tissue cutting/processing, we also evaluated axon regeneration using unbiased 3D microscopy. *Thy1*-GFP-M transgenic mice in which ~10% of neurons, including DRG neurons, express GFP (Feng et al., 2000) were divided into stress or no-stress groups; all mice then received a sciatic nerve crush. Whole sciatic nerves were collected and cleared (3DISCO; Ertürk et al., 2012) and all axons were quantified using fluorescence light sheet microscopy and Imaris 3D Visualization Software (Bitplane, Oxford Instruments; Fig. 7*E*,*F*; Movies 1, [2]; Ertürk et al., 2012; Renier et al., 2014). Axon profiles in the distal nerve segment were quantified at 14 dpi, a time when injured axons and myelin debris are normally cleared from the injury site (Vargas et al., 2010). This provides a "clean" background for assessing total numbers of regenerating axons. Using this approach, we found that stress increased the overall number of GFP+ axons ~2-fold throughout the 5-cm distance examined distal to the crush site when compared with injured nerves from ns mice (Fig. 7*G-I*). Together, these data show that acute stress augments regenerative growth of injured peripheral nerves *in vivo*.

Discussion

Novel data in this report show that stress and GCs enhance the sprouting and regenerative growth of adult sensory axons, *in vitro* and *in vivo*. Using *in silico* modeling strategies, we identified several TFs and RAGs with GC-response elements and show that some of these genes are regulated by stress via GR-dependent mechanisms.

In the brain, stress and GCs enhance structural plasticity (e.g., dendrite growth/retraction), neurogenesis, memory, and neuronal excitability (Imperato et al., 1991; Kaufer et al., 1998; Kirby et al., 2013). Because hippocampal neurons express high basal levels of GRs, they are thought to be uniquely responsive to circulating GCs (Fuxe et al., 1985; Reul and De Kloet, 1985). However, our data indicate that sensory neurons also express high GR levels, more so than hippocampal neurons, and are exquisitely sensitive to stress and circulating GCs.

The axon growth promoting effects of stress and GCs are reminiscent of the effects of injuring the peripheral branch of DRG sensory neurons (McQuarrie and Graf-

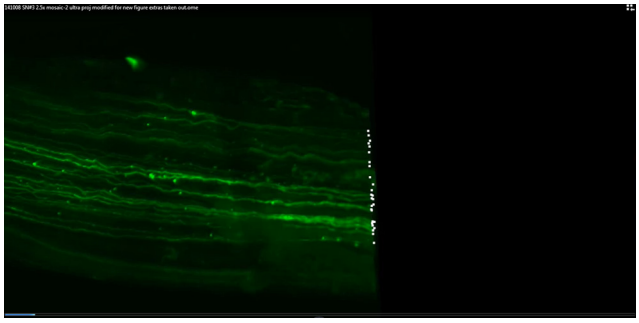

Movie 1. Thy1-GFPM sciatic nerve in a ns mouse 14 d after crush injury. Green fibers are axons distal to the crush site. The box through the image shows an area quantified using the spots algorithm (Imaris), and white dots show the results of the algorithm, indicating counted axons. [View online]

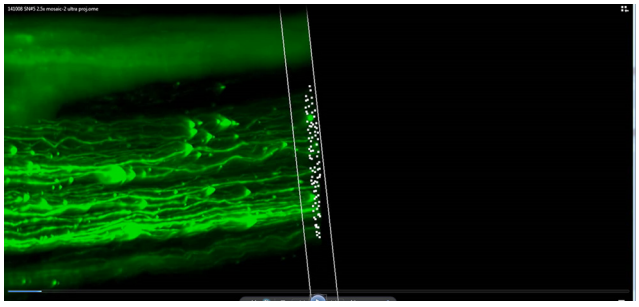

Movie 2. Thy1-GFPM sciatic nerve in a stressed mouse 14 d after injury crush injury. Green fibers are axons distal to the crush site. The box through the image shows an area quantified using the spots algorithm (Imaris) and white dots show the results of the algorithm, indicating counted axons. [View online]

stein, 1973; Lasek et al., 1984; Smith and Skene, 1997). These "conditioning" lesions promote axon growth in part by activating developmental growth programs and transcription of RAGs (McQuarrie and Grafstein, 1973; Bonilla et al., 2002; Qiu et al., 2005). Because GRs are TFs that are activated by stress (or circulating GCs), we hypothesized that they would similarly enhance RAG expression, providing an explanation for the ability of stress/GCs to augment sensory axon growth *in vitro* and *in vivo*. Instead, we found that although stress enhances axon outgrowth through GC-GR-dependent mechanisms, these effects likely occur rapidly (immediately poststress) and do not involve transcriptional regulation of traditional RAGs. Indeed, stress only modestly increased expression of a subset of RAGs and such changes typically took 1-3 d. Other traditional RAGs (e.g., *Jun*, *Il6*, *Atf3*) were repressed. GR repression of *Il6* and *Atf3* is consistent with previous studies of *Il6* in COS cells and *Atf3* in macrophages (Verhoog et al., 2011; Chinenov et al., 2014). Moreover, when paired with a conditioning lesion, stress partially inhibited or delayed the injury-evoked increases in RAG expression. Thus, GRs likely power sensory axon growth by controlling the transcription of genes that are constitutively expressed *in vivo* by DRG neurons and not traditional RAGs. Using *in silico* analyses, we identified several candidate genes (Tables 1-3) and demonstrate that the CCAAT/enhancer binding proteins (*Cebp*) are at least one gene family that is positively regulated by GC-GR binding.

Cebps are transcriptional regulators of cellular differentiation, terminal function and responses to inflammation and tissue injury (Poli, 1998; Ménard et al., 2002; Calella et al., 2007). In the nervous system, *Cebpb* expression increases in regenerating facial motor neurons and may control the expression of other genes necessary for axon growth (Nadeau et al., 2005). Loss of *Cebpd* function in mice delays regeneration of injured peripheral nerve (Lopez de Heredia and Magoulas, 2013). Although we did not prove that *Cebps* are responsible for the axon growth promoting effects of stress, our data do show that *Cebpa* and *Cebpb* expression are induced by acute stress and that GC-GR interactions drive expression of *Cebp-a*, *-b*, and *-d*. Although these data implicate *Cebps* as regulators of stress-induced neurite growth, additional studies are needed to unequivocally prove a causal role for these TFs in regulating stress-induced axon plasticity.

The current experiments focused on the effects of GC-GR interactions in adult sensory neurons. Other neurons and glia also express GRs, and in response to injury or stress, GCs undoubtedly affect structure and function in these cells. As an example, after spinal cord injury basal GR expression increases in spinal neurons, but it is not known how GR activation influences neural plasticity (Ferrini et al., 1993; Wang et al., 2004). GR activation in microglia and astrocytes can induce or repress cell cycle, proliferation, and inflammatory processes (Crossin et al., 1997; Hwang et al., 2006; Frank et al., 2010; Carter et al., 2012); and GC-GR interactions influence Schwann cell proliferation (Neuberger et al., 1994), which is required for efficient peripheral nerve regeneration (Hall, 1986). In future studies, conditional targeting of GRs will reveal the range of mechanisms and cell types that underlie stress-enhanced growth and plasticity after nerve injury.

The current data may have broad clinical implications, since stress is ubiquitous and synthetic corticosteroids are widely used as anti-inflammatory agents to treat various diseases in animals and humans. Perhaps most notable are the consequences that the present data could have for the diagnosis and treatment of neuropathic pain. Consider that in animal models of nerve injury or inflammatory pain (Wang et al., 2004; Khasar et al., 2005, 2008; Alexander et al., 2009), stress and GCs exacerbate pain behaviors and these effects are reversed by GR inhibitors. Stress can also elicit or exacerbate pain in human disease (Ashkinazi and Vershinina, 1999; Turner et al., 2002; Greco et al., 2004; Nicholson and Martelli, 2004; DeLeo, 2006). The mechanisms underlying chronic pain are complex and incompletely understood; however, a number of publications indicate that nerve injury causes functional reorganization of injured sensory neurons, with sprouting of sensory axons, mostly nociceptive afferents, into the superficial layers of the spinal cord dorsal horn (Woolf et al., 1992; Okamoto et al., 2001; Ondarza et al., 2003; Hughes et al., 2008; Woodbury et al., 2008; Zhang et al., 2015). Perhaps stress and GCs exacerbate this nerve-injury induced phenomenon of axonal plasticity within the superficial dorsal horn. We also cannot rule out the possibility that stress-induced increases in GCs could enhance pain respones by increasing axonal sprouting ("plasticity") in other areas of the CNS involved in sensory processing (e.g., nucleus cuneatus and gracilis; Persson et al., 1995; Ma and Bisby, 1998, 2000). Overall, our data highlight the importance of stress and GCs as novel behavioral and circulating modifiers of sensory neuron plasticity and should prompt new discussion about whether the inflammation associated with pain should be treated with steroids.

References

Abe N, Borson SH, Gambello MJ, Wang F, Cavalli V (2010) Mammalian target of rapamycin (mTOR) activation increases axonal growth capacity of injured peripheral nerves. J Biol Chem 285: 28034–28043. CrossRef Medline

Ahmed T, Frey JU, Korz V (2006) Long-term effects of brief acute stress on cellular signaling and hippocampal LTP. J Neurosci 26:3951–3958. CrossRef Medline

Alexander JK, DeVries AC, Kigerl KA, Dahlman JM, Popovich PG (2009) Stress exacerbates neuropathic pain via glucocorticoid and NMDA receptor activation. Brain Behav Immun 23:851–860. CrossRef Medline

Ashkinazi IY, Vershinina EA (1999) Pain sensitivity in chronic psychoemotional stress in humans. Neurosci Behav Physiol 29:333–337.

Bonilla IE, Tanabe K, Strittmatter SM (2002) Small proline-rich repeat protein 1A is expressed by axotomized neurons and promotes axonal outgrowth. J Neurosci 22:1303–1315. Medline

Cafferty WBJ, Gardiner NJ, Gavazzi I, Powell J, McMahon SB, Heath JK, Munson J, Cohen J, Thompson SWN (2001) Leukemia inhibitory factor determines the growth status of injured adult sensory neurons. J Neurosci 21:7161–7170.

Calella AM, Nerlov C, Lopez RG, Sciarretta C, von Bohlen und Halbach O, Bereshchenko O, Minichiello L (2007) Neurotrophin/Trk receptor signaling mediates C/EBPalpha, -beta and NeuroD

recruitment to immediate-early gene promoters in neuronal cells and requires C/EBPs to induce immediate-early gene transcription. Neural Dev 2:4. CrossRef Medline

Campbell G, Hutchins K, Winterbottom J, Grenningloh G, Lieberman AR, Anderson PN (2005) Upregulation of activating transcription factor 3 (ATF3) by intrinsic CNS neurons regenerating axons into peripheral nerve grafts. Exp Neurol 192:340–347. CrossRef Medline

Carter BS, Meng F, Thompson RC (2012) Glucocorticoid treatment of astrocytes results in temporally dynamic transcriptome regulation and astrocyte-enriched mRNA changes in vitro. Physiol Genomics 44:1188–1200. CrossRef Medline

Chinenov Y, Coppo M, Gupte R, Sacta MA, Rogatsky I (2014) Glucocorticoid receptor coordinates transcription factor-dominated regulatory network in macrophages. BMC Genomics 15:656 CrossRef Medline

Cho Y, Sloutsky R, Naegle KM, Cavalli V (2013) Injury-induced HDAC5 nuclear export is essential for axon regeneration. Cell 155:894–908. CrossRef Medline

Crossin KL, Tai MH, Krushel LA, Mauro VP, Edelman GM (1997) Glucocorticoid receptor pathways are involved in the inhibition of astrocyte proliferation. Proc Natl Acad Sci USA 94:2687–2692. Medline

De Kloet E, Vreugdenhil E, Oitzl M, Joëls M (1998) Brain corticosteroid receptor balance in health and disease. Endocr Rev 19:269–301. CrossRef Medline

Decosterd I, Woolf CJ (2000) Spared nerve injury: an animal model of persistent peripheral neuropathic pain. Pain 87:149–158. Medline

DeLeo JA (2006) Basic science of pain. J Bone Joint Surg Am 88 [Suppl 2]:58–62. CrossRef Medline

DeLeón M, Coveñas R, Chadi G, Narváez JA, Fuxe K, Cintra A (1994) Subpopulations of primary sensory neurons show coexistence of neuropeptides and glucocorticoid receptors in the rat spinal and trigeminal ganglia. Brain Res 636:338–342. Medline

Ertürk A, Mauch CP, Hellal F, Förstner F, Keck T, Becker K, Jährling N, Steffens H, Richter M, Hübener M, Kramer E, Kirchhoff F, Dodt HU, Bradke F (2012) Three-dimensional imaging of the unsectioned adult spinal cord to assess axon regeneration and glial responses after injury. Nat Med 18:166–171. CrossRef

Feng G, Mellor RH, Bernstein M, Keller-Peck C, Nguyen QT, Wallace M, Nerbonne JM, Lichtman JW, Sanes JR (2000) Imaging neuronal subsets in transgenic mice expressing multiple spectral variants of GFP. Neuron 28:41–51. Medline

Ferrini M, González S, Antakly T, De Nicola AF (1993) Immunocytochemical localization of glucocorticoid receptors in the spinal cord: effects of adrenalectomy, glucocorticoid treatment, and spinal cord transection. Cell Mol Neurobiol 13:387–397. Medline

Fitzsimons CP, van Hooijdonk LW, Schouten M, Zalachoras I, Brinks V, Zheng T, Schouten TG, Saaltink DJ, Dijkmans T, Steindler DA, Verhaagen J, Verbeek FJ, Lucassen PJ, de Kloet ER, Meijer OC, Karst H, Joels M, Oitzl MS, Vreugdenhil E (2013) Knockdown of the glucocorticoid receptor alters functional integration of newborn neurons in the adult hippocampus and impairs fear-motivated behavior. Mol Psychiatry 18:993–1005. CrossRef Medline

Frank MG, Miguel ZD, Watkins LR, Maier SF (2010) Prior exposure to glucocorticoids sensitizes the neuroinflammatory and peripheral inflammatory responses to E. coli lipopolysaccharide. Brain Behav Immun 24:19–30. CrossRef

Frey D, Laux T, Xu L, Schneider C, Caroni P (2000) Shared and unique roles of CAP23 and GAP43 in actin regulation, neurite outgrowth, and anatomical plasticity. J Cell Biol 149:1443–1454. Medline

Fuxe K, Wikström A, Okret S, Agnati L, Härfstrand A, Zu ZY, Granholm L, Zoli M, Vale W, Gustafsson JA (1985) Mapping of glucocorticoid receptor immunoreactive neurons in the rat tel- and diencephalon using a monoclonal antibody against rat liver glucocorticoid receptor. Endocrinology 117:1803–1812. CrossRef

Gensel JC, Schonberg DL, Alexander JK, McTigue DM, Popovich PG (2011) Semi-automated Sholl analysis for quantifying changes in growth and differentiation of neurons and glia. J Neurosci Methods 190:71–79. CrossRef

Greco CM, Rudy TE, Manzi S (2004) Effects of a stress-reduction program on psychological function, pain, and physical function of systemic lupus erythematosus patients: a randomized controlled trial. Arthritis Rheum 51:625–634. CrossRef Medline

Hajji OE, Nobuta H, Waschek JA, Armstrong BD, Abad C, Chhith S, Cheung-Lau G (2008) Impaired nerve regeneration and enhanced neuroinflammatory response in mice lacking pituitary adenylyl cyclase activating peptide. Neuroscience 151:63–73. CrossRef Medline

Hall SM (1986) The effect of inhibiting Schwann cell mitosis on the re-innervation of acellular autografts in the peripheral nervous system of the mouse. Neuropathol Appl Neurobiol 12:401–414. Medline

Hughes AS, Averill S, King VR, Molander C, Shortland PJ (2008) Neurochemical characterization of neuronal populations expressing protein kinase C gamma isoform in the spinal cord and gracile nucleus of the rat. Neuroscience 153:507–517. CrossRef Medline

Hwang IK, Yoo K-Y, Nam YS, Choi JH, Lee IS, Kwon Y-G, Kang T-C, Kim Y-S, Won MH (2006) Mineralocorticoid and glucocorticoid receptor expressions in astrocytes and microglia in the gerbil hippocampal CA1 region after ischemic insult. Neurosci Res 54: 319–327. CrossRef Medline

Imperato A, Puglisi-allegra S, Casolini P, Angelucci L (1991) Changes in brain dopamine and acetylcholine release during and following stress are independent of the pituitary-adrenocortical axis. Brain Res 538:111–117. CrossRef

Joëls M, Velzing E, Nair S, Verkuyl JM, Karst H (2003) Acute stress increases calcium current amplitude in rat hippocampus: temporal changes in physiology and gene expression. Eur J Neurosci 18: 1315–1324. Medline

Kaufer D, Seidman S, Soreq H (1998) Acute stress facilitates long-lasting changes in cholinergic gene expression. Nature 38:373–377.

Kerr DS, Campbell LW, Thibaultt O, Landfield PW (1992) Hippocampal glucocorticoid receptor activation enhances voltage-dependent. Proc Natl Acad Sci USA 89:8527–8531. Medline

Khasar SG, Burkham J, Dina OA, Brown AS, Bogen O, Alessandri-Haber N, Green PG, Reichling DB, Levine JD (2008) Stress induces a switch of intracellular signaling in sensory neurons in a model of generalized pain. J Neurosci 28:5721–5730. CrossRef

Khasar SG, Green PG, Levine JD (2005) Repeated sound stress enhances inflammatory pain in the rat. Pain 116:79–86. CrossRef Medline

Kirby ED, Muroy SE, Sun WG, Covarrubias D, Leong MJ, Barchas LA, Kaufer D (2013) Acute stress enhances adult rat hippocampal neurogenesis and activation of newborn neurons via secreted astrocytic FGF2. Elife 2:e00362. CrossRef Medline

Lasek J, Oblinger MM, Lasek RJ (1984) A conditioning lesion of the peripheral axons of dorsal root ganglion cells accelerates regeneration of only their peripheral axons. J Neurosci 4:1736–1744.

Li C-L, Li K-C, Wu D, Chen Y, Luo H, Zhao J-R, Wang S-S, Sun M-M, Lu Y-J, Zhong Y-Q, Hu X-Y, Hou R, Zhou B-B, Bao L, Xiao H-S, Zhang X (2015) Somatosensory neuron types identified by high-coverage single-cell RNA-sequencing and functional heterogeneity. Cell Res 1–20.

Lopez de Heredia L, Magoulas C (2013) Lack of the transcription factor C/EBPδ impairs the intrinsic capacity of peripheral neurons for regeneration. Exp Neurol 239:148–157. CrossRef Medline

Lupien SJ, de Leon M, de Santi S, Convit A, Tarshish C, Nair NP, Thakur M, McEwen BS, Hauger RL, Meaney MJ (1998) Cortisol levels during human aging predict hippocampal atrophy and memory deficits. Nat Neurosci 1:69–73. CrossRef

Ma W, Bisby MA (2000) Partial sciatic nerve ligation induced more dramatic increase of neuropeptide Y immunoreactive axonal fibers in the gracile nucleus of middle-aged rats than in young adult rats. J Neurosci Res 60:520–530. CrossRef Medline

Ma W, Bisby MA (1998) Partial and complete sciatic nerve injuries induce similar increases of neuropeptide Y and vasoactive intes-

tinal peptide immunoreactivities in primary sensory neurons and their central projections. Neuroscience 86:1217–1234. Medline
McMahon SB, Armanini MP, Ling LH, Phillips HS (1994) Expression and coexpression of Trk receptors in subpopulations of adult primary sensory neurons projecting to identified peripheral targets. Neuron 12:1161–1171. Medline
McQuarrie IG, Grafstein B (1973) Axon outgrowth enhanced by a previous nerve injury. Arch Neurol 29:53–55. Medline
Ménard C, Hein P, Paquin A, Savelson A, Yang XM, Lederfein D, Barnabé-Heider F, Mir AA, Sterneck E, Peterson AC, Johnson PF, Vinson C, Miller FD (2002) An essential role for a MEK-C/EBP pathway during growth factor-regulated cortical neurogenesis. Neuron 36:597–610. CrossRef
Michaelevski I, Segal-Ruder Y, Rozenbaum M, Medzihradszky KF, Shalem O, Coppola G, Horn-Saban S, Ben-Yaakov K, Dagan SY, Rishal I, Geschwind DH, Pilpel Y, Burlingame AL, Fainzilber M (2010) Signaling to transcription networks in the neuronal retrograde injury response. Sci Signal 3:ra53. CrossRef Medline
Mitra R, Sapolsky RM (2008) Acute corticosterone treatment is sufficient to induce anxiety and amygdaloid dendritic hypertrophy. Proc Natl Acad Sci USA 105:5573–5578. CrossRef Medline
Moore DL, Blackmore MG, Hu Y, Kaestner KH, Bixby JL, Lemmon VP, Goldberg JL (2009) KLF family members regulate intrinsic axon regeneration ability. Science 326:298–301. CrossRef Medline
Nadeau S, Hein P, Fernandes KJ, Peterson AC, Miller FD (2005) A transcriptional role for C/EBP beta in the neuronal response to axonal injury. Mol Cell Neurosci 29:525–535. CrossRef Medline
Neuberger TJ, Kalimi O, Regelson W, Kalimi M, De Vries GH (1994) Glucocorticoids enhance the potency of Schwann cell mitogens. J Neurosci Res 38:300–313. CrossRef Medline
Neumann S, Woolf CJ (1999) Regeneration of dorsal column fibers into and beyond the lesion site following adult spinal cord injury. Neuron 23:83–91. Medline
Nicholson K, Martelli MF (2004) The problem of pain. J Head Trauma Rehabil 19:2–9. CrossRef
Okamoto M, Baba H, Goldstein PA, Higashi H, Shimoji K, Yoshimura M (2001) Functional reorganization of sensory pathways in the rat spinal dorsal horn following peripheral nerve injury. J Physiol 532:241–250. Medline
Ondarza AB, Ye Z, Hulsebosch CE (2003) Direct evidence of primary afferent sprouting in distant segments following spinal cord injury in the rat: colocalization of GAP-43 and CGRP. Exp Neurol 184:373–380. Medline
Persson JKE, Lindh B, Elde R, Robertson B, Rivero-Melián C, Eriksson NP, Hökfelt T, Aldskogius H (1995) The expression of different cytochemical markers in normal and axotomised dorsal root ganglion cells projecting to the nucleus gracilis in the adult rat. Exp Brain Res 105:331–344.
Poli V (1998) The role of C/EBP isoforms in the control of inflammatory and native immunity functions. J Biol Chem 273:29279–29282. Medline
Qiu J, Cafferty WB, McMahon SB, Thompson SW (2005) Conditioning injury-induced spinal axon regeneration requires signal transducer and activator of transcription 3 activation. J Neurosci 25:1645–1653. CrossRef Medline
Renier N, Wu Z, Simon DJ, Yang J, Ariel P, Tessier-Lavigne M (2014) iDISCO: a simple, rapid method to immunolabel large tissue samples for volume imaging. Cell 159:896–910. CrossRef Medline
Reul J, De Kloet E (1985) Two receptor systems for corticosterone in rat brain: microdistribution and differential occupation. Proc Natl Acad Sci USA 117:6174–6177. CrossRef
Revest J-MM, Di Blasi F, Kitchener P, Rougé-Pont F, Desmedt A, Turiault M, Tronche F, Piazza PV, Rouge-Pont F (2005) The MAPK pathway and Egr-1 mediate stress-related behavioral effects of glucocorticoids. Nat Neurosci 8:664–672. CrossRef Medline
Riccardi C, Zollo O, Nocentini G, Bruscoli S, Bartoli A, D'Adamio F, Cannarile L, Delfino D, Ayroldi E, Migliorati G (2000) Glucocorticoid hormones in the regulation of cell death. Therapie 55:165–169. Medline
Sapolsky RM, Krey LC, McEwen BS (1984) Glucocorticoid-sensitive hippocampal neurons are involved in terminating the adrenocortical stress response. Proc Natl Acad Sci USA 81:6174–6177. CrossRef
Schneider CA, Rasband WS, Eliceiri KW (2012) NIH Image to ImageJ: 25 years of image analysis. Nat Methods 9:671–675. Medline
Seijffers R, Mills CD, Woolf CJ (2007) ATF3 increases the intrinsic growth state of DRG neurons to enhance peripheral nerve regeneration. J Neurosci 27:7911–7920. CrossRef Medline
Shields SD, Eckert WA 3rd, Basbaum AI (2003) Spared nerve injury model of neuropathic pain in the mouse: a behavioral and anatomic analysis. J Pain 4:465–470. Medline
Shin JE, Geisler S, Diantonio A (2014) Dynamic regulation of SCG10 in regenerating axons after injury. Exp Neurol 252:1–11. CrossRef Medline
Shin JE, Miller BR, Babetto E, Cho Y, Sasaki Y, Qayum S, Russler EV, Cavalli V, Milbrandt J, DiAntonio A (2012) SCG10 is a JNK target in the axonal degeneration pathway. Proc Natl Acad Sci USA 109:E3696–E3705. CrossRef
Smith DS, Skene JH (1997) A transcription-dependent switch controls competence of adult neurons for distinct modes of axon growth. J Neurosci 17:646–658. Medline
Stam FJ, MacGillavry HD, Armstrong NJ, de Gunst MCM, Zhang Y, van Kesteren RE, Smit AB, Verhaagen J (2007) Identification of candidate transcriptional modulators involved in successful regeneration after nerve injury. Eur J Neurosci 25:3629–3637. CrossRef Medline
Turner JA, Jensen MP, Warms CA, Cardenas DD (2002) Catastrophizing is associated with pain intensity, psychological distress, and pain-related disability among individuals with chronic pain after spinal cord injury. Pain 98:127–134. Medline
Usoskin D, Furlan A, Islam S, Abdo H, Lönnerberg P, Lou D, Hjerling-Leffler J, Haeggström J, Kharchenko O, Kharchenko PV, Linnarsson S, Ernfors P (2015) Unbiased classification of sensory neuron types by large-scale single-cell RNA sequencing. Nat Neurosci 18:145–153. CrossRef Medline
Vargas ME, Watanabe J, Singh SJ, Robinson WH, Barres BA (2010) Endogenous antibodies promote rapid myelin clearance and effective axon regeneration after nerve injury. Proc Natl Acad Sci USA 107:11993–11998. CrossRef Medline
Verhoog NJD, Du Toit A, Avenant C, Hapgood JP (2011) Glucocorticoid-independent repression of tumor necrosis factor (TNF) α-stimulated Interleukin (IL)-6 expression by the glucocorticoid receptor: a potential mechanism for protection against an excessive inflammatory response. J Biol Chem 286:19297–19310. CrossRef
Vyas A, Mitra R, Shankaranarayana Rao BS, Chattarji S, Rao BSS (2002) Chronic stress induces contrasting patterns of dendritic remodeling in hippocampal and amygdaloid neurons. J Neurosci 22:6810–6818.
Wang S, Lim G, Zeng Q, Sung B, Ai Y, Guo G, Yang L, Mao J (2004) Expression of central glucocorticoid receptors after peripheral nerve injury contributes to neuropathic pain behaviors in rats. J Neurosci 24:8595–8605. CrossRef Medline
Wasserman W, Sandelin A (2004) Applied bioinformatics for the identification of regulatory elements. Nat Rev Genet 5:276–287.
Watanabe Y, Gould E, McEwen BS (1992) Stress induces atrophy of apical dendrites of hippocampal CA3 pyramidal neurons. Brain Res 588:341–345. Medline
Wei P, Inamdar N, Vedeckis WV (1998) Transrepression of c-jun gene expression by the glucocorticoid receptor requires both AP-1 sites in the c-jun promoter. Mol Endocrinol 12:1322–1333. CrossRef Medline
Woodbury CJ, Kullmann FA, McIlwrath SL, Koerber HR (2008) Identity of myelinated cutaneous sensory neurons projecting to nociceptive laminae following nerve injury in adult mice. J Comp Neur 508:500–509. CrossRef Medline
Woolf CJ, Shortland P, Coggeshall RE (1992) Peripheral nerve injury triggers central sprouting of myelinated afferents. Nature 355:75–78. CrossRef Medline

Wu D, Huang W, Richardson PM, Priestley JV, Liu M (2008) TRPC4 in rat dorsal root ganglion neurons is increased after nerve injury and is necessary for neurite outgrowth. J Biol Chem 283:416–426. CrossRef Medline

Yang CH, Huang CC, Hsu KS (2004) Behavioral stress modifies hippocampal synaptic plasticity through corticosterone-induced sustained extracellular signal-regulated kinase/mitogen-activated protein kinase activation. J Neurosci 24:11029–11034. CrossRef Medline

Zhang Y, Chen Y, Liedtke W, Wang F (2015) Lack of evidence for ectopic sprouting of genetically labeled Aβ touch afferents in inflammatory and neuropathic trigeminal pain. Mol Pain 11:18. CrossRef Medline